TECTONOPHYSICS

Tectonophysics 332 (2001) 115–141

www.elsevier.com/locate/tecto

# Thermally softened continental extensional zones (arcs and rifts) as precursors to thickened orogenic belts

A.B. Thompson[a,*], K. Schulmann[b], J. Jezek[c], V. Tolar[b]

[a]Departement Erdwissenschaften, ETH Zurich CH-8092, Switzerland
[b]Department of Petrology and Structural Geology, Charles University, Prague, Czech Republic
[c]Department of Applied Mathematics, CZ-128 43, Charles University, Prague, Czech Republic

**Abstract**

Intra-continental deformation of soft zones during continental collision requires weak continental lithosphere which is able to be shortened across considerable width during later convergence. This enables significant thickening with formation of an orogenic root. We have examined models with a history of lithospheric thinning by pure shear during an earlier phase of intra-continental extension with associated heating. Geologically this situation is appropriate to intra-continental rifts and back-arc basins.

If thinning of elevated thermal structure is decoupled from the thinning of lithology then a weak (soft) lower crust and sub-arc/rift mantle result. This weak structure has a favoured rheology for subsequent convergent thickening while the lithosphere is still hot. These regions are associated with formation of granulites and metamorphic assemblages typical of high-temperature/low-pressure (HT/LP).

If convergence starts while the heat input is still active then the failed rifts and arcs are shut off by lateral wedging of the hard lower crust and upper mantle of shoulder regions into the softened arc/rift domain. Such sites are ideal for the formation and for the exhumation of metamorphic core complexes. Subsequent thickening during convergence leads to HT eclogites when the previous arc/rift was hot and to medium-T eclogites for a thickened "standard" geotherm. These $P$–$T$ paths are counter-clockwise and their shapes are strongly dependent on the amount of previous thinning and type of initial geotherm.

If the compression starts long after cessation of the extensional event and associated thermal anomaly, then the geotherm of the extended area relaxes and the whole region hardens. In this case, no homogeneous thickening occurs and deep continental roots cannot form. 

*Keywords*: lithosphere rheology; orogenic root; prograde metamorphism; continental extension; continental thickening

## 1. Introduction

Previous considerations of continental collision which modelled doubling the thickness of a standard continental thickness of 35 km with a standard geotherm, have shown that the metamorphic rocks should record pressures commonly much higher than observed (England and Thompson, 1984; Jamieson et al., 1998). Furthermore, homogeneous ductile deformation of the lithosphere is difficult because thickening of lithosphere with a standard geotherm results in deep thick zones with brittle rheologies (Ranalli and Murphy, 1987; Cloethingh et al., 1995).

For homogeneous thickening of continental crust in convergent orogenic zones to occur to a significant extent the continental crust needs to be thermally

* Corresponding author. Tel.: +41-1-6321111; fax: +41-1-6321088.

*E-mail address:* alan@erdw.ethz.ch (A.B. Thompson).

0040-1951/01/$ - see front matter 
PII: S0040-1951(00)00252-3

softened before thickening (Oxburgh, 1982; Buck and Toksoez, 1983; Thompson, 1989a,b). The commonest cause of thermal weakening is upraised asthenosphere beneath continental rifts and arcs. Continental rifts are active when they result from impingement of mantle plumes on the base of the lithosphere, or passive when remote forces pull continental plates apart (Sengor and Burke, 1978). Continental back arcs become extended in response to the roll-back of subduction, and upflowing mantle induces extension and increased heat flow and magmatism (Dewey and Burke, 1973; Grocott et al., 1994; Tatsumi and Kimura, 1991; Ziegler et al., 1998). Recently extended continental domains are still weak after the cessation of an extensional event and during the waning of the thermal anomaly (Buck and Toksoez, 1983; Parsons et al., 1992; Bertotti et al., 1997; Hopper and Buck, 1998). The sub-arc/rift mantle also forms a part of this softened, easily deformable, 'continental asthenosphere' which can be shortened horizontally if convergence occurs soon afterwards (see also Kooi and Cloetingh, 1989). Thus, a high rheological contrast between soft and deformable warm 'continental asthenosphere' and adjacent stiff and cold blocks of converging continental lithosphere is a favourable condition for thickening of continents (Tommasi and Vauchez, 1997; Vauchez et al., 1998).

A similar setting was also successfully used by Merle and Guillier (1989) in analogue models for the progressive thickening of extended domains. In their model the maximum depth of the thickened sub-arc/rift Moho was chosen to be 70 km, but in fact this would be limited by the depth to which the rigid subcontinental mantle can be compressed vertically and laterally to host the deepening continental root. Three important questions still to be answered are: (i) At what depth does the deepening of original extended domains cease? (ii) What is the mechanical role of the sub-arc/rift mantle during intra-continental convergence? (iii) What is the pressure and temperature evolution during thickening of previously extended domains?

This paper presents a numerical thermomechanical investigation of the progressive thickening of previously thinned continental domains with plane-strain geometry. The role of sub-arc/rift mantle, as a major mechanical factor blocking the downward movement during convergence, is assessed from the rheological and thermal point of view. We have not specifically considered here the processes of mechanical coupling within the continental crust nor at the Moho. We consider here that extension is passive, i.e. remote plate forces control the thermal and geological developments of intra-continental arcs and rifts.

## 2. Possible deformation of standard continents

Continents of standard thickness (35 km to Moho), with cold to standard geotherms (see Table A1) and standard lithology (upper crust of average quartz rheology to 20 km, lower crust of felsic or mafic rheology from 20 to 35 km) are not easily deformable (Kusznir and Park, 1986; Cloetingh and Burov, 1996). The average stratified crust exhibits alternating brittle and viscous (in the sense of Schmid and Handy, 1991; but often referred to as 'ductile' in the sense of Ranalli and Murphy, 1987) layers. Homogeneous thickening can occur only in viscous material, while the brittle layers will host thrust faults when the crust is in compression.

The tectonic style is influenced by the type of geotherm. A cold geotherm results in narrow and localised zones of weakness in brittle crust and crustal thickening uses heterogeneous thin weak zones as shears. Therefore heterogeneous thrust thickening is the overall mechanism of crustal thickening for cold and standard geotherms. This type of thickening is responsible for the further modification of the thermal structure of convergent orogens due to the development of a saw-tooth-like perturbed geotherm. The thickened domains harden during this process (as shown by Ranalli and Murphy, 1987; Ellis, 1988). Hotter geotherms result in thicker ductile layers and eventually can permit ductile thickening of continental crust by homogenous viscous flow deformation. A similar reasoning is used by Merle and Guillier (1989) and Chery et al. (1991) in their analogue and kinematic modelling of homogeneous deformation of orogenic roots.

Extensive homogeneous thickening of the crust is therefore only possible if the average thickness of crustal ductile layers is great, or can be increased (England and Houseman, 1985; England, 1987; Cloethingh et al., 1995; Royden, 1996). These circumstances occur most likely in crust with substantial thickness of quartz-rich lithologies, and in crust that has been recently thermally softened. Continental crust of standard thickness represents a weak heterogeneity only if it possesses a hotter geotherm, or weaker integrated strength, than the adjacent lithosphere. Thus regions that have recently undergone intra-continental extension homogeneously provide the most favourable circumstances for crust thickening. We do not discuss here any localised thickening mechanisms, such as stacking of layers with different rheologies (Ranalli and Murphy, 1987; Ellis, 1988), effects of underthrusting (or subduction, e.g. Jamieson et al., 1998), or influence of precollisional crustal and mantle anisotropies (Vauchez et al., 1998).

## 3. Mechanical conditions in intra-continental rifts and arcs

Inherited rheology influences the dynamics of the continental root formation in former intra-continental extended domains following changes in plate motion (Oxburgh, 1982; Cloethingh et al., 1995). The effects of initial depth to Moho and thermal state of an original extended domain determines the effectiveness of far field stresses and associated strain rates in the process of thickening of softened extended zones (Allemand and Brun, 1991). In our model (see Appendix A), the pre-convergence rheology is defined as a function of thickness of individual crustal layers and geotherms of the extended domains and adjacent continental shoulder lithosphere. Horizontal stretching and thinning can be instantaneous or occur over a time interval. In both cases, horizontal stretching results in immediate upraising of the sub-arc/rift asthenosphere. Importantly, shortly after thinning, the sub-arc/rift domain is softened and can be homogeneously deformed and thickened during a subsequent episode of compression (see Thompson, 1989a,b; Ziegler et al., 1995; Ziegler et al., 1998). Geologically this transition from continental thinning to thickening may reflect an increase in convergence velocity or change in plate motion direction relative to the position of the former active arc/rift.

The thermal and mechanical interplay at various times in this history of compression of extended (thermally and lithologically thinned) lithosphere is the subject of our modelling here.

First, we consider that the deep heat source is deactivated immediately after thinning and thus the sub-arc/rift domain cools through time (following Morgan and Ramberg, 1987). This will manifest as the dying of volcanism — which can act as a time (and perhaps even as depth) marker for the waning of the sub-arc/rift heat source. Later we examine examples where the deep heat source is not deactivated and continues to function during the thickening event.

Even though we are mainly interested in the sub-arc/rift region, the lower crust of the shoulders adjacent to the rift are important to maintain the integrity of the arc/rift, to initiate rift-flank faults and to the subsequent deformation if convergence develops (Ziegler et al., 1995). For this reason we have considered several different initial geotherms and two different lower crustal materials, both for the extended domain and for the adjacent shoulders. Fig. 1 shows a profile for the two-dimensional (2D) crustal thinning, and the coupled perturbations of lithology and thermal structure for a thinning factor, $\beta = 2$. This type of pure shear extension parallel to the lithological layering yields only absolute upper bounds on the lithospheric strength (Handy, personal communication). Thus the different layer strengths which affect the depth of necking (Cloethingh et al., 1995), and development of shear instabilities during layer-parallel extension in an anisotropic system (Cosgrove, 1997), are not included here.

Lithospheric thinning in continental rifts is associated with coeval attenuation of lithospheric mantle and crust. The strength of the lithosphere in extended domains depends on the rate of crustal ($\beta$) and lithospheric mantle ($\delta$) extension (McKenzie, 1978). Greater amounts of lithospheric thinning ($\delta$) than crustal thinning ($\beta$) result in the development of a weak heterogeneity, whereas equal thinning ($\delta = \beta$) results in the development of a stiff domain below the arc/rift (Quinlan, 1988; Vauchez et al., 1998).

Lithospheric thinning can be viewed in the first instance as a one-dimensional (1D) vertical process when the width of the arc/rift is greater than the initial depth to Moho. The thinning process of extension is mainly controlled by the thermal structure and the rheology of the ultramafic mantle lithosphere (see also Cloethingh et al., 1995). To determine favourable conditions for lithospheric thinning a large range of input parameters were considered.

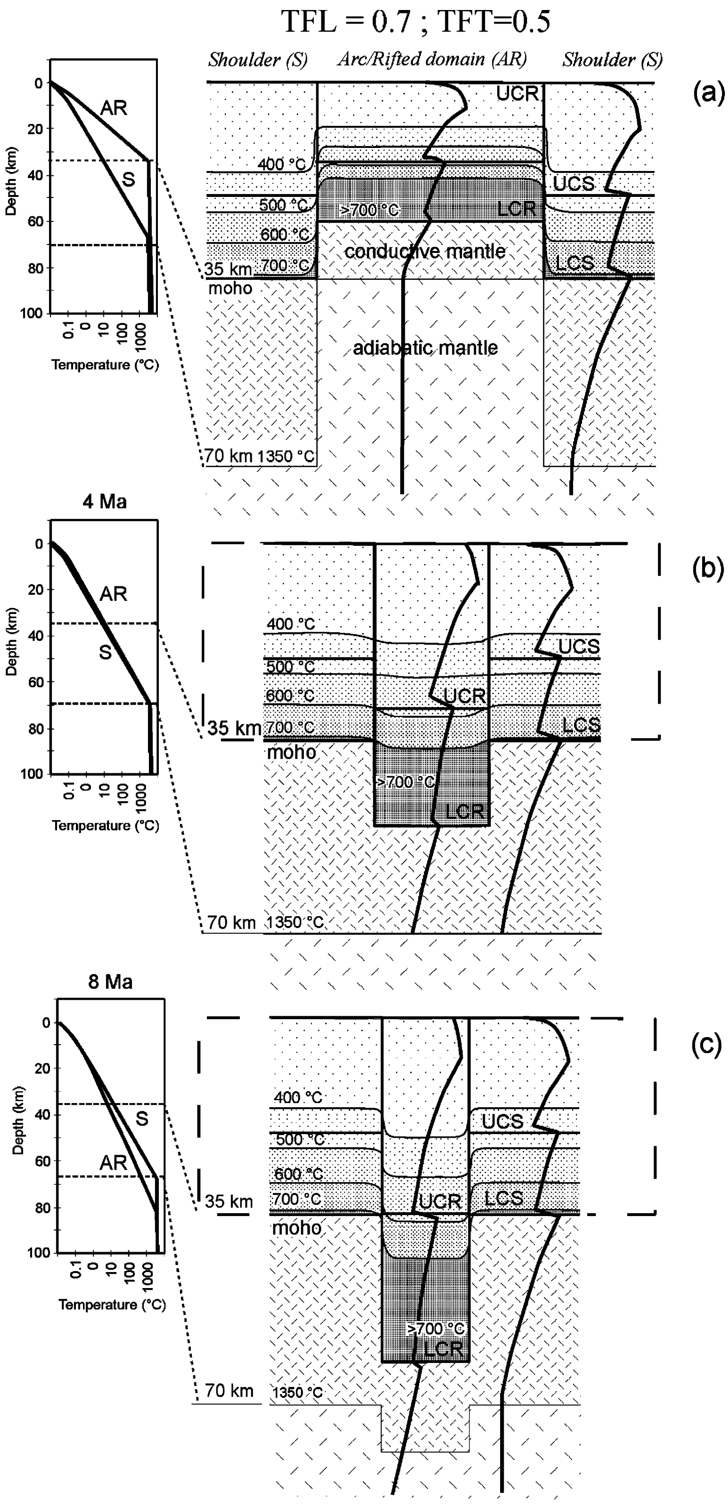
TFL = 0.7 ; TFT=0.5
Shoulder (S)
Arc/Rifted domain (AR)
Shoulder (S)
(a)
(b)
(c)
4 Ma
8 Ma
Depth (km)
Temperature (°C)
AR
S
UCR
UCS
LCR
LCS
400 °C
500 °C
600 °C
700 °C
>700 °C
35 km
moho
70 km
1350 °C
conductive mantle
adiabatic mantle

Table 1
Lithosphere rheology and geotherm parameters used in the modelling

| Layer (km) | | $n$ | $A$ (MPa$^{-n}$ s$^{-1}$) | $Q$ (J mol$^{-1}$) | $\beta$ | $\rho$ (kg cm$^{-3}$) | lam |
|---|---|---|---|---|---|---|---|
| Quartzite (dry) | 20 | 2.4 | $6.31\times10{-6}$ | 156 000 | 1.2 | 2600 | 0.36 |
| Diabase | 15 | 3.4 | $2.02\times10^{-4}$ | 260 000 | 1.2 | 2900 | 0.36 |
| Quartz diorite | 15 | 2.4 | $1.26\times10^{-3}$ | 219 000 | 1.2 | 2900 | 0.36 |
| Olivine | 115 | 3 | $4.00\times10^{+6}$ | 540 000 | 1.2 | 3100 | 0.36 |
| *Geotherm parameters* | | | | | | | |
| A | 2 μW.m$^{-3}$ | | | | | | |
| D | 15 km | | | | | | |
| K | 2.25 W m$^{-1}$ K$^{-1}$ | | | | | | |
| C | 1000 J kg$^{-1}$ K$^{-1}$ | | | | | | |
| Qm hot | 40 mW m$^{-2}$ | | | | | | |
| Qm standard | 30 mW m$^{-2}$ | | | | | | |
| Qm cold | 20 mW m$^{-2}$ | | | | | | |

## 4. Rheological modelling of the mechanical evolution of the lithosphere

We have constructed yield strength envelopes (YSE) for pre-convergence states in unextended continents (future arc/rift shoulders) and extended domains (see Appendix A). For the construction of YSE for unextended continents we have used three types of geotherms similar to those defined by England and Thompson (1984) and Ranalli and Murphy (1987). To constrain YSE, we used yield strength equations relating stress needed for a permanent deformation at depth (see Appendix A). The brittle properties of the rocks (Navier–Coulomb law using Byerlee's constants) depend more on pressure than on the temperature and rock type. Because we neither account for the temperature and pressure dependence of these constants, nor the frictional behaviour, the brittle layers will be slightly thicker than calculated here (Handy, 1989).

The mechanical properties of a deformed lithospheric domain in the ductile field are described by empirical constitutive relations expressing the yield stress limits of quartz for upper crust, diorite for the intermediate composition lower crust, diabase for mafic lower crust, and olivine (similar to dunite) for mantle, as a function of temperature and strain rate (Goetze and Evans, 1979; Kirby, 1983; Ranalli, 1986; Ranalli and Murphy, 1987; Paterson and Luan, 1990).

All thermal and flow-law parameters used for modelling are presented in Table 1. For unextended lithosphere, we assumed the crust to be 35 km thick, composed of 20 km of upper crust (dry quartz), 15 km of lower crust (quartz diorite for felsic lower crust, diabase for mafic lower crust). Mantle, represented by olivine, has been assigned a thickness of 115 km for the models.

The integrated strength values (ISV) of the individual lithospheric columns inside and outside the compressed arc/rift are calculated according to England (1987). These values are used to demonstrate

Fig. 1. Block diagrams showing structure and evolution of unperturbed continent (shoulder, S, Moho at 35 km) which has been instantaneously thinned to 70% in an arc or rift (AR) domain, and then gradually thickened during convergence. During thinning the thermal structure is uncoupled from the lithology, the abbreviation TFT = 0.7, TFL = 0.5 means that the lithology is thinned to 70% of its former thickness and the thermal structure is thinned to half thickness. In (a) the initial 'hot' geotherms (Table 1) for both domains are shown in the left panel. The corresponding initial and post-thinning Yield Strength Envelopes (YSE) for the rheology/lithology of 20 km upper crust (UC) = quartz; 20–35 km felsic lower crust (LC) = diorite; olivine mantle, (Table 1) are shown by the thick crenulated lines for unperturbed (S = shoulder) and thinned ard/rift (AR) domains. The small difference in strength near the depth of the thinned Moho is responsible for the different development of continental lithosphere in thermal histories of crustal thinning followed by thickening. (b) and (c), Geothermal and rheological structure after 4 (b) and 8 (c) Ma into thickening history. The 1350°C isotherm for the mantle adiabat can be viewed as separating overlying conductive from underlying convective thermal regimes.

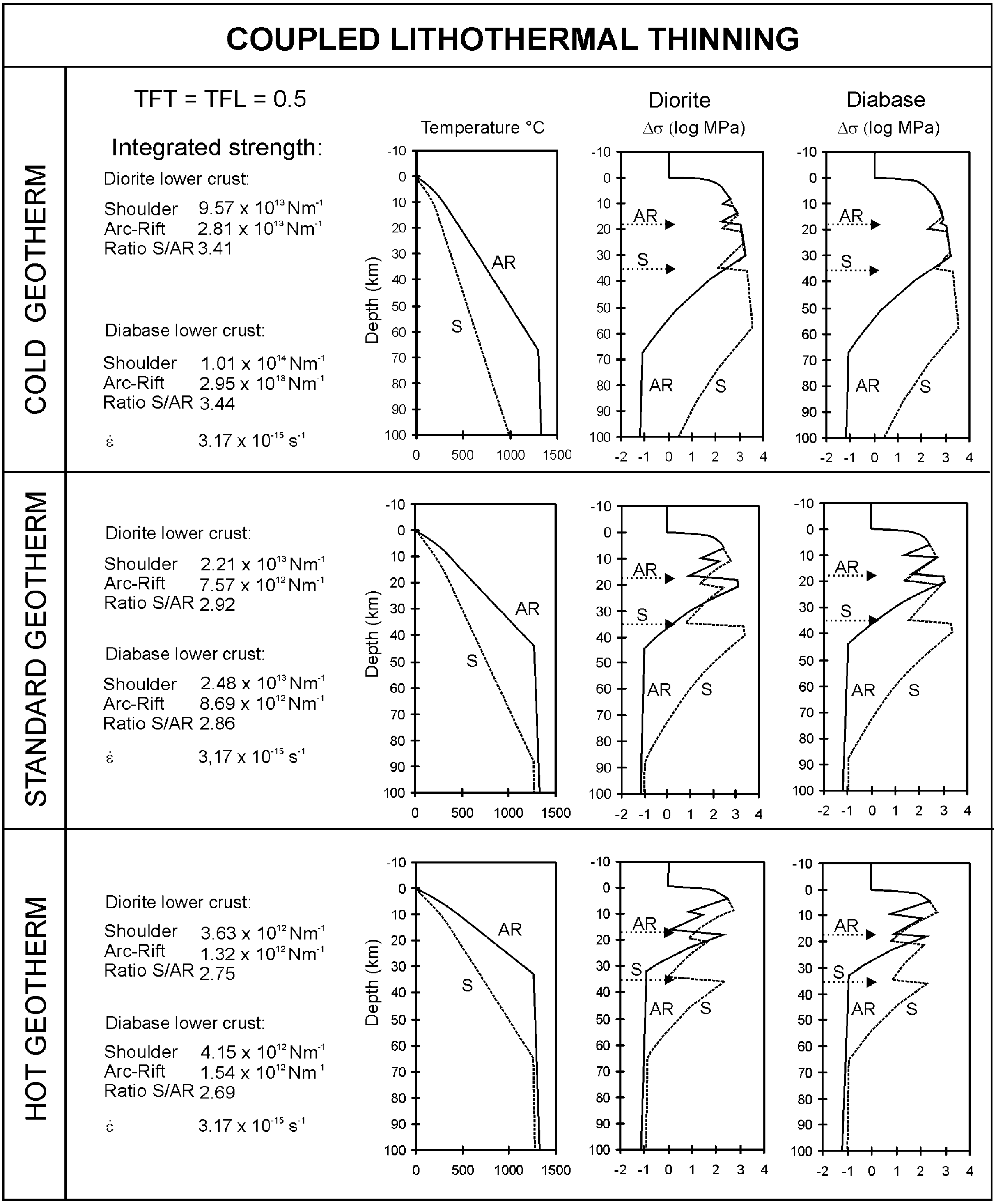
COUPLED LITHOTHERMAL THINNING
TFT = TFL = 0.5
Integrated strength:
COLD GEOTHERM
Diorite lower crust:
Shoulder 9.57 x 10^13 Nm^-1
Arc-Rift 2.81 x 10^13 Nm^-1
Ratio S/AR 3.41
Diabase lower crust:
Shoulder 1.01 x 10^14 Nm^-1
Arc-Rift 2.95 x 10^13 Nm^-1
Ratio S/AR 3.44
ε̇ 3.17 x 10^-15 s^-1
STANDARD GEOTHERM
Diorite lower crust:
Shoulder 2.21 x 10^13 Nm^-1
Arc-Rift 7.57 x 10^12 Nm^-1
Ratio S/AR 2.92
Diabase lower crust:
Shoulder 2.48 x 10^13 Nm^-1
Arc-Rift 8.69 x 10^12 Nm^-1
Ratio S/AR 2.86
ε̇ 3,17 x 10^-15 s^-1
HOT GEOTHERM
Diorite lower crust:
Shoulder 3.63 x 10^12 Nm^-1
Arc-Rift 1.32 x 10^12 Nm^-1
Ratio S/AR 2.75
Diabase lower crust:
Shoulder 4.15 x 10^12 Nm^-1
Arc-Rift 1.54 x 10^12 Nm^-1
Ratio S/AR 2.69
ε̇ 3.17 x 10^-15 s^-1
Temperature °C
Depth (km)
Diorite
Δσ (log MPa)
Diabase
Δσ (log MPa)
AR
S

the relative weakness of compressed arc/rift with respect to adjacent continent.

The rheology of extended domains with respect to adjacent continents has been compared at various geotherms and for two compositions of lower crust. For the case where the extended domain is weaker than the adjacent continental lithosphere, its rheology has also been compared for several stages of thickening of extended lithosphere. The thinning and subsequent thickening of lithological layers of extended domains is represented in our model by a thinning/thickening factor for lithology, TFL (see Appendix A). We use this factor to describe, in a unique way, both the processes of thinning and thickening. As a thinning factor, our TFL is less than one and is equal to the reciprocal value of the factor $\beta$ (McKenzie, 1978). For the case of equal thinning of crust and the mantle $\delta$ equals $\beta$. Thickening by homogeneous plane-strain is represented by the factor TFL greater than one. The thinning and thickening factor for temperature (TFT, see Appendix A) is used to derive any transient modelled geotherm from an initial geotherm, and has similar meaning to TFL. For our calculations it has been assumed that each increment of thinning/thickening is isostatically compensated. We assume that in nature the thermal boundary layer regions are narrow compared to the width of the arc/rift. Therefore 1D modelling is adequate for the length scales considered here in the centre of the modelled domain.

### 4.1. The strength of thinned lithosphere in which lithosphere thickness and thermal structure are coupled

For initial conditions of our model, we assume that the lithosphere is thinned to half of the original thickness (Moho from 35 to 17.5 km). This type of ‘coupled’ homogeneous pure shear thinning of lithological layers occurs simultaneously with the thinning of isotherms. We have examined thinning of lithospheres with different thermal structure (cold, standard and hot geotherms) and with different lower crustal compositions (diorite, diabase). This procedure simulates rapid extension of the lithosphere, during which the thermal structure is passively transported upwards together with lithological layers, but without a significant upwelling of the asthenospheric mantle. Fig. 2 shows the changes in lithospheric strength after thinning (horizontal stretching) in comparison with the non-stretched, adjacent lithosphere (35 km thick continental shoulders to the arc/rift) with respect to different types of geotherms and relative to the initial configuration shown in Fig. 1. Immediately after thinning, the extended lithosphere is about three times weaker (e.g. the ratio of integrated strengths of shoulder to rift is about 3.44, 2.86, and 2.69, for the three geotherms in Fig. 2).

Closer examination of Figs. 1 and 2 show that the sub-continental mantle is significantly stronger than the sub-arc/rift mantle for the depth interval from 35 to 63, 35 to 88 and 35 to 120 km, for hot, standard and cold initial geotherms, respectively. The mantle beneath the extended domain with the ‘standard’ initial geotherm, and granodioritic lower crust, is significantly stronger than the lower crust and part of the continental upper-crust of the continental shoulder, in the depth interval from 17 to 28 km, whereas the lower and upper crust of the extended domain is weaker than the upper crust of the continental shoulder.

The relationships between YSE of continent and rift are only slightly different for the mafic lower crust. Here, the sub-arc/rift mantle is stronger than the lower part of the adjacent shoulder upper crust, and the sub-arc/rift lower crust shows almost equal strength to the shoulder upper crust. For the hot geotherm, the sub-rift mantle is stronger than the upper continental crust only in a narrow interval between 23 and 17 km for dioritic lower crust and between 20 and 17 for mafic lower crust. Similar analysis of strength profiles for a cold geotherm shows that the upper mantle and lower crust of the rifted domain are stronger than the lower and upper crust of the continental shoulder in the range from 35

Fig. 2. Coupled thermal and rheological structure (TFT = TFL = 0.5) for unperturbed (S = shoulder) and thinned (AR = arc/rift) continental lithosphere for $\beta = 2$, for three geotherms (Table 1). Also shown are corresponding yield strength envelopes ($\Delta\sigma$ in MPa, $\dot{\epsilon} = 3 \times 10^{-15}\ \mathrm{s}^{-1}$) for two cases of lower crustal rheology/lithology (20–35 km depth, felsic = Diorite, mafic = Diabase), and the location of the Moho. The “step” in mantle rheology only reflects the sharp change in the geothermal structure as used here.

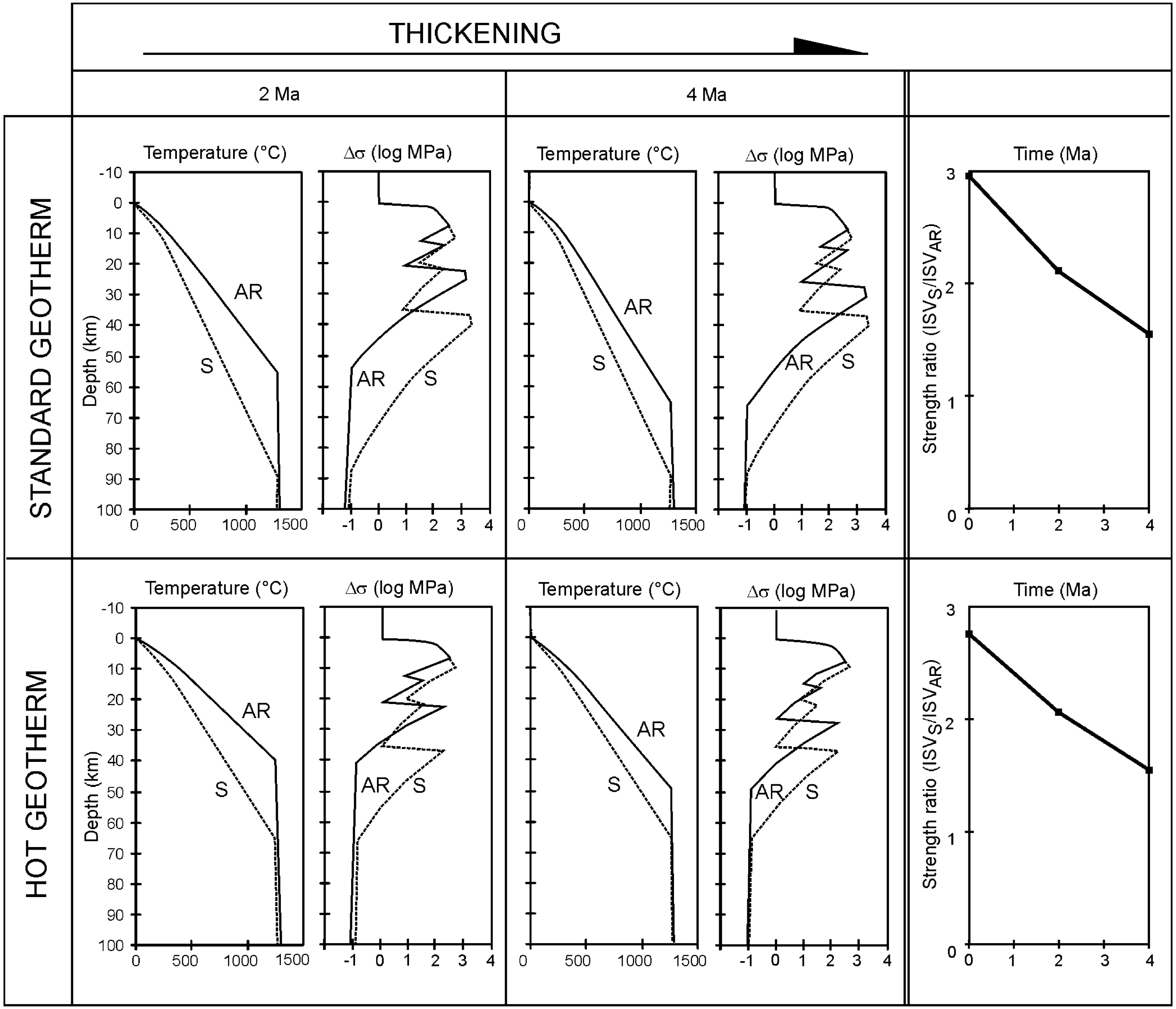
THICKENING
2 Ma
4 Ma
STANDARD GEOTHERM
HOT GEOTHERM
Temperature (°C)
Δσ (log MPa)
Depth (km)
AR
S
Time (Ma)
Strength ratio (ISVS/ISVAR)

to 17 km. The ratio of integrated strength values ($ISV_S/ISV_{AR}$) indicates that the continental shoulder lithosphere is stronger than the arc/rift lithosphere. Especially in the case of a mafic lower crust, the main contribution to the regional strength of the lithosphere is influenced by very strong sub-continental mantle. However above 35 km, the extended lithosphere is stronger than the adjacent continental crust for standard and cold geotherms (shaded regions in the $\Delta\sigma$ — depth diagrams in Fig. 2), and slightly weaker for the hot geotherm. In agreement with a prediction by Oxburgh (1982), the thickness of this region progressively increases with time during cooling, so that the sub-arc/rift mantle will become stronger than the adjacent continental lower crust. This strength distribution will play a significant role in tectonic style during the compression of continental domains which contain rifted regions.

### *4.2. Possible thickening of extended zones with coupled thermal and lithological structures*

The strength profiles of thinned lithosphere with hot and standard geotherms show a narrow layer of strong sub-rift mantle that is stronger than the adjacent shoulder lithosphere. We can imagine that the strong sub-rift mantle layers are small compared to the whole lithospheric structure, and that the rifted domain shows bulk strength less than that of shoulder lithosphere. These conditions may allow limited horizontal shortening of weaker arc/rift regions.

We will now examine a possible thickening of an extended domain characterised by coupled thinning of temperature and lithology (TFT = TFL). The thickening process of the extended lithosphere is simulated by multiplying the initial values of TFT and TFL stepwise by a factor of 1.22, which simulates the homogeneous pure shear thickening with a time increment of 2 Ma for a zone 100 Ma wide and for a plate velocity of 1 cm/year. These simulations are performed for both standard and hot geotherms, and for dioritic and diabasic lower crust.

Our calculations show that after 2 Ma of thickening the strength of the crustal part of the sub-arc/rift lithosphere becomes equal to or even higher than that of the adjacent crustal part of the shoulder lithosphere (Fig. 3). At this time the sub-arc/rift lithosphere is about two-times weaker than continental lithosphere. After 4 Ma of thickening, a very strong sub-arc/rift lower crust and mantle layers develop adjacent to the weaker upper crust and lower crust of the continental shoulder lithosphere, respectively. The strength ratio, $ISV_S/ISV_{AR}$ is 1.5 for both standard and hot geotherms. This indicates a tendency towards equal strength for both continental shoulder and sub-arc/rift lithospheres after only a very short period of thickening (Fig. 3). We suggest that the root cannot thicken further due to the presence of a rigid sub-continental mantle and a rigid sub-arc/rift lithosphere higher in the column. This configuration may lead to horizontal shortening of the sub-arc/rift mantle by strong continental mantle and lateral wedging of strong sub-arc/rift layers into adjacent continental crust.

Our analysis shows that the compression of continental arcs and rifts, where thermal and lithological thinning (TFL = TFT) were coupled, would not result in homogeneous thickening of the weaker extended zone, and hence would never lead to the development of an orogenic root. Limited thickening is possible in the range of several kilometers, leading to the development of alternating strong layers opposite softer parts of adjacent lithosphere. These strong layers result in lateral wedging of the sub-continental mantle into weak sub-arc/rift mantle, and the opposite-direction wedging of a sub-arc/rift mantle chisel into a weaker continental lower crust. The thickness of such sub-rift mantle wedges decreases from cold to hot geotherms, as will be discussed elsewhere.

## 5. Lithosphere thinning in which thickness and thermal structure are not coupled

Lithospheric thinning is often related to the upwelling of mantle material. The total lithospheric thinning is often greater than the crustal thinning so that the case $\delta \gg \beta$ in many continental arcs and rifts results in a

Fig. 3. 'Standard' and 'Hot' geotherm model of homogeneous pure shear thickening of thinned lithosphere, for coupled TFT = TFL = 0.5 ($\beta = 2$), at 2, 4 Ma. Right side diagrams show the evolution of the ratio of $ISV_S$ (shoulder, diorite lower crust) /$ISV_{AR}$ (arc/rift root, diorite lower crust), during thickening following coupled extensional thinning of an arc (or rift).

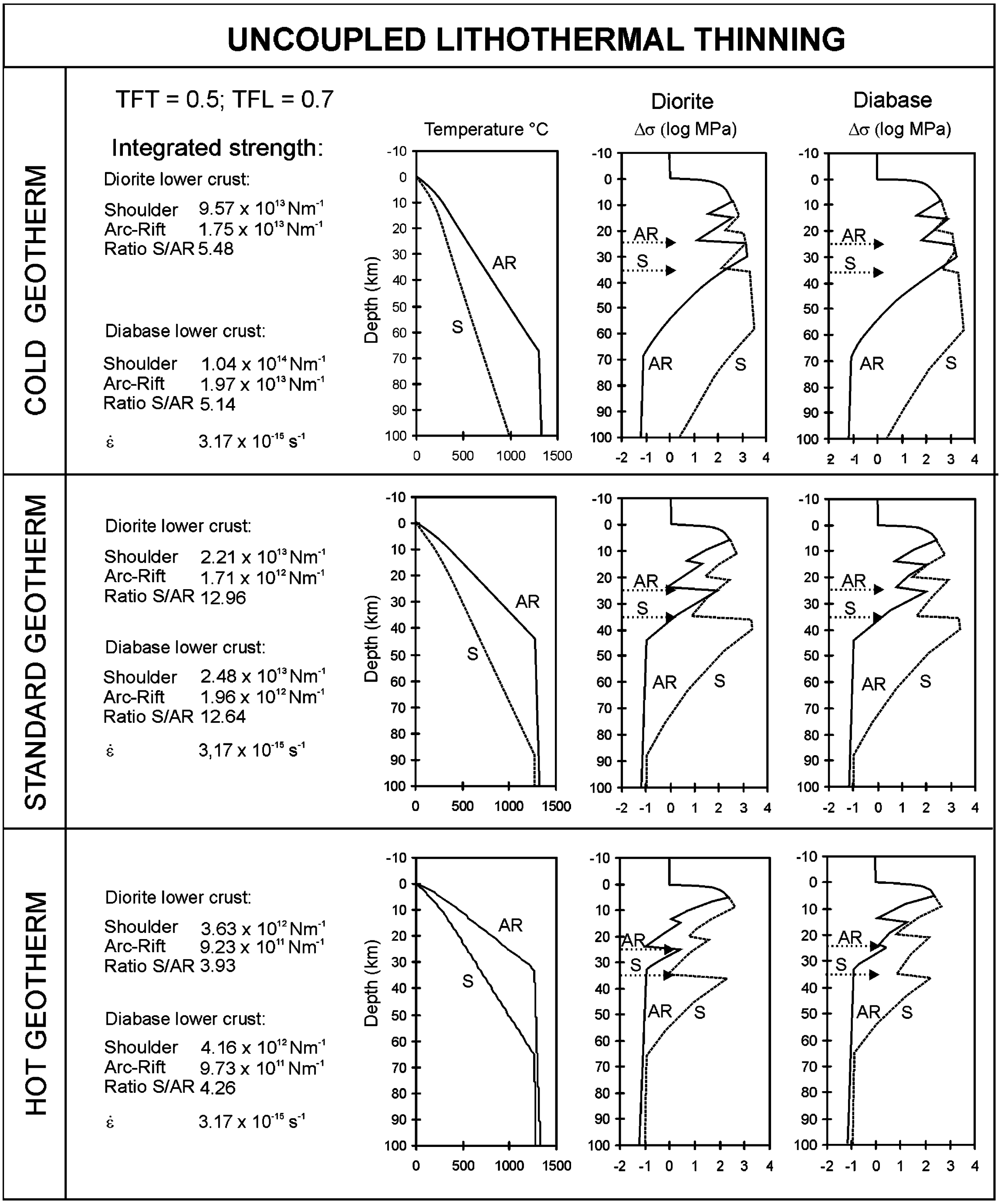


Fig. 4. Uncoupled thermal and rheological structure for unperturbed (S = shoulder) and thinned (AR = arc/rift) continental lithosphere for $\beta = 2$, for three geotherms (Table 1). The abbreviation TFT = 0.5 for TFL = 0.7 means that the lithology is thinned to 70% of the unperturbed thickness (35 km) and the thermal structure thinned to 50%, this simulates addition of heat compared to coupled case of Fig. 2. Also shown are corresponding yield strength envelopes ($\Delta\sigma$ in M Pa, $\dot{\epsilon} = 3 \times 10^{-15}\ \mathrm{s}^{-1}$), for two cases of lower crustal rheology/lithology (20–35 km depth, felsic = Diorite, mafic = Diabase), and the location of the Moho.

significant decrease in strength of the sub-arc/rift lithosphere (Tommasi and Vauchez, 1997). Several models of lithospheric extension with $\delta > \beta$, a condition favouring the development of important weak heterogeneities, are listed by Vauchez et al. (1998). A weakened sub-arc lithosphere is maintained during the prolonged magmatic activity in back-arc basins that is related to the melting of a mantle wedge above a subduction zone. However, the cooling of the arc/rift with $\delta > \beta$ is responsible for strengthening of the lithosphere in a similar way to the previous case of coupled thinning. The rate of strengthening of the arc/rift lithosphere may be diminished by several factors such as thermal blanketing by sediments, or thermally unequilibrated adjacent lithosphere that cools together with the arc or rift (Vauchez et al., 1998).

Lithospheric extension with $\delta > \beta$ can be successfully modelled using 'decoupled' TFT and TFL values. For the case of greater thermal than lithological thinning ($TFT = 0.5 < TFL = 0.7$), the extended domain is weak and can be horizontally shortened immediately following extension. Relevant here is the time period over which the extended domain remains warm and soft after cessation of the thermal anomaly. Such conditions are met in several intra-continental rifts such as the East African and Baikal rifts, Rhine Graben, Salton Sea Trough, and the Tyrrhenian sea (Bassi et al., 1993). Measured heat flow in active and Cenozoic rifts show values of surface heat flow between 110–130 mW/m$^2$ (Rhine Graben — Glahn and Granet, 1993; Salton Trough — McDowell and Elders, 1983). Seismic surveys suggest an exceptionally elevated Moho for these domains. In the case of the Rhine Graben and the Pannonian Basin (Lankreijer et al., 1997) the Moho reaches 25 km, and in the Salton Trough it reaches 21 km in Imperial Valley (Lachenbruch et al., 1985). In the case of the Rhine Graben, intrusions of ultramafic (shoshonitic) magmas occurred during Cenozoic times and are apparently related to the peak period of rifting (Glahn and Granet, 1993). Similarly, a massive intrusion of mafic gabbroic magmas is proposed at a depth of 15–21 km in Imperial Valley (Salton Trough). The Pannonian Basin, a typical continental back-arc basin, is characterised by a relatively thin crust (25–28 km), high heat flow values (90–100 mW/m$^2$) and very thin lithosphere (50–80 km, Lankreijer et al., 1997). Both types of arc/rift structures show exceptional thinning of the lithosphere and regions associated with important mafic to ultramafic magmatism. Closer examination of these lithospheric structures, however, shows that the thermal anomaly at the surface appears not to correspond exactly to that which originates by coupled thinning ($TFT = TFL$) associated with lithospheric stretching and thinning characterised by $\delta = \beta$. Surface heat flow of 100 mW/m$^2$ indicates temperatures around 1000°C at a depth of 25 km (Lachenbruch et al., 1985). In both cases of continental rifts and back-arc basins, an additional heat input exists, probably located at significant depth in the lithosphere (ultramafic magmas originate perhaps near 100 km, e.g. Green, 1991).

For a Moho depth of 25 km, a TFL of 0.7 corresponds to thinning of a lithosphere of 35 km original thickness. A temperature of 1000°C at a depth of 25 km corresponds to a TFT value of 0.5 applied to the original pre-thinning, hot geotherm (Fig. 4). A hot initial geotherm is not unrealistic when recent surface heat flow measurements of Variscan Saxothuringian (60–70 mW/m$^2$), or the Moldanubian part of the Bohemian Massif (40–60 mW/m$^2$), are taken into account (Cermák et al., 1993; Cloetingh and Burov, 1996).

Physical processes, which influence the thermal structure independently of lithosphere thinning, would result in the thermal profiles being more elevated than the lithological profile. Such events include the intrusion of magma (Thompson and Gibson, 1994), upraised asthenosphere following delamination, or the incursion of a thermal plume beneath intra-continental arcs or rifts. The objective of these considerations is to understand the mechanisms which produce completely softened sub-arc/rift mantle relative to that of adjacent continental shoulder. As shown above this cannot be achieved when lithological and thermal thinning are coupled. Decoupling during thinning, so that thermal structure is elevated higher than lithology, requires introduction of heat in addition to the advected geotherm.

## 6. Strength of arcs and rifts with decoupled thinning of lithology and thermal structure

In our models, the TFL (thinning factor for lithology) for development of extended domains was taken as 0.7. This value derives from the natural rifts and arcs mentioned above, where the arc/rift Moho is at 25 km, the shoulder Moho is at 35 km

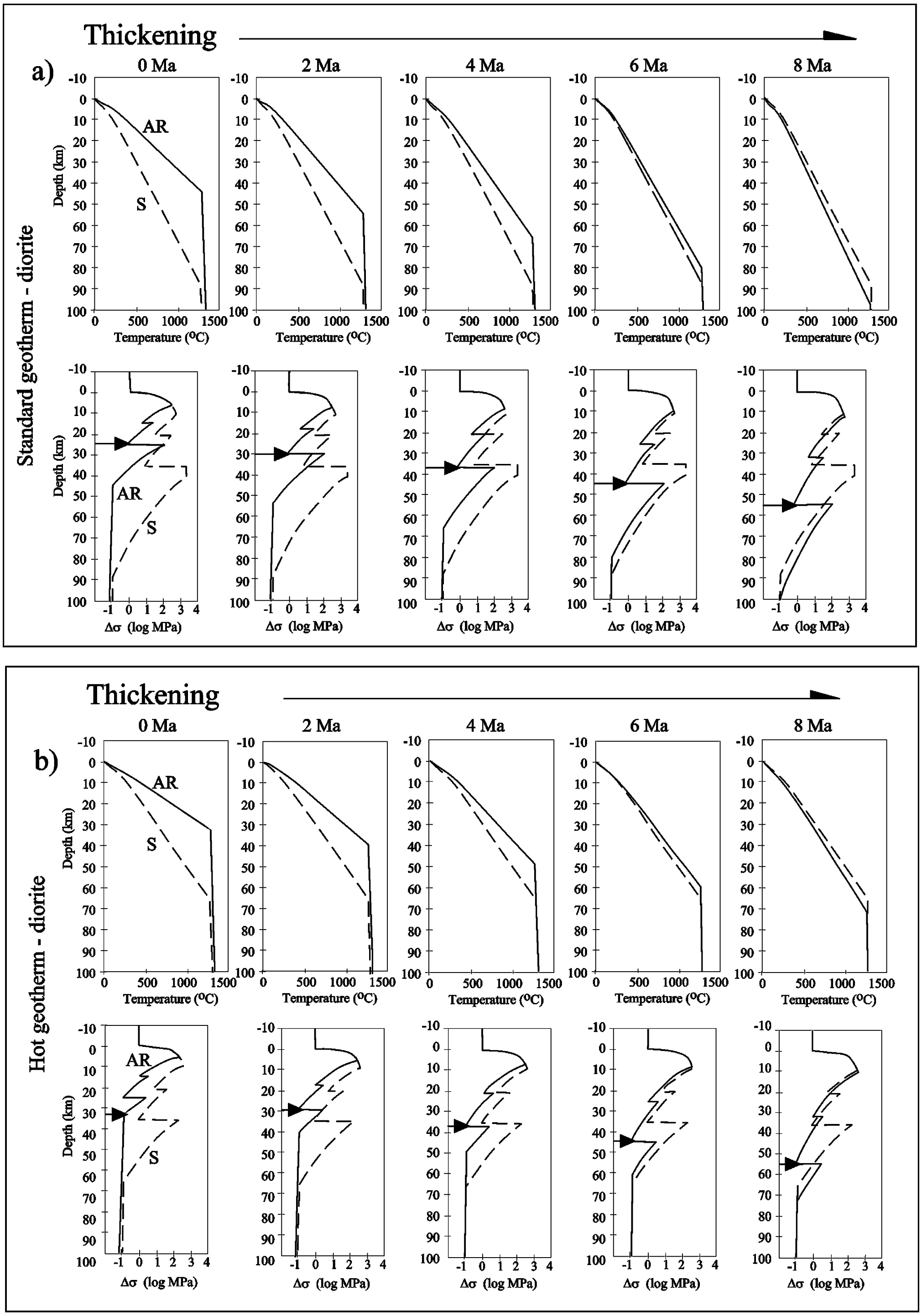


Fig. 5. (a) 'Standard' geotherm model of progressive thickening of thinned lithosphere, for decoupled TFT = 0.5 and TFL = 0.7 ($\beta = 1.43$), at 0, 2, 4, 6, 8 Ma. into the thickening history. The thermal structure and YSE's for the deepening of the upper/lower crustal and Moho (arrowed) boundaries are shown for unperturbed (S = shoulder) and thinned (AR = arc/rift) continental lithosphere, for felsic = diorite, lower crustal rheology (20–35 km depth). (b) 'Hot' geotherm–diorite model of progressive thickening of thinned lithosphere, other factors as in (a).

(20/35 = 0.7). Thus the Moho after extension is at a depth of 24.5 km, and the base of the upper crust at 14 km (Fig. 3). Hot and standard geotherms for extended domains have a TFT factor of 0.5 (1000°C at 25 km, see above). Initially, we compare $YSE_{AR}$ and $ISV_{AR}$ of extended arc/rift regions with $YSE_S$ and $ISV_S$ of adjacent continental shoulder lithosphere. Comparative YSE values in Fig. 4 are constructed for various geotherms of thinned and unthinned lithosphere.

An important feature of these YSE values is that for the initial hot and standard initial geotherms, the whole lithosphere below the arc/rift is weaker than adjacent continental lithosphere. For the standard geotherm the extended domain is about 12 times weaker than the adjacent continental shoulder lithosphere. A similar situation is also predicted for extended lithosphere with a hot geotherm; the sub-arc/rift lithosphere is approximately 4 times weaker than the continental shoulder.

In the case of 'decoupled' thinning of lithosphere with dioritic lower crust and a cold geotherm, the sub-arc/rift mantle is still stronger than the adjacent continental shoulder lower crust. Mafic lower crust and its sub-arc/rift mantle have similar strengths as the continental shoulder lower and upper crust. The integrated strength values for continental and sub-arc/rift lithosphere show that the shoulder is at least 5 times stronger than the sub-arc/ rift (Fig. 4). However, the strength of the upper 35 km of sub-arc/ rift lithosphere is either of equal strength to or stronger than the adjacent continental shoulder. This means that the homogeneous thickening of thinned lithosphere with a cold geotherm remains impossible.

## 7. Thickening of thinned lithosphere

For hot and standard geotherms the thinned lower crust and sub-arc/rift mantle are consistently weaker than the adjacent continental shoulder lithosphere. This facilitates homogeneous thickening. We will now consider thickening of an extended domain that is characterised by 'decoupled' thinning of temperature and lithology (TFT = TFL) following cessation of the thermal anomaly beneath the arc/rift. In this model, multiplying initial values of TFT and TFL simulates the thickening process of the weakened extended lithosphere stepwise by a factor of 1.22. This simulates the thickening associated with the passive transportation of rocks at constant temperature. This mechanism represents the most rapid thickening process for which the thermal equilibration of a perturbed geotherm is fully neglected. No extra heat is added during this particular thickening process. This stage in the mechanism resembles the case of homogeneous thickening of the entire lithosphere (England and Thompson, 1984, Fig. 3c and f).

Figs. 4 and 5 show the evolution of $YSE_S$ for hot and standard geotherms after subsequent increments of TFL representing two million years for a strain rate of $\dot{\epsilon}3.17 \times 10^{-15}\ s^{-1}$ ($\sim$0.1 $Ma^{-1}$, i.e. corresponding to the shortening of a 100 km wide zone by 1 cm/ year).

### 7.1. Formation of an orogenic root at constant strain-rate

After 4 Ma, the Moho and base of the arc/rift lower crust are at about the same depth as in the continental shoulder lithosphere (Figs. 5 and 6a). For both geotherms the thickened extended domain is still hotter than the continental shoulder domain. Consequently, the whole-extended lithosphere is weaker than the adjacent continental lithosphere: more than twice as weak for the hot initial geotherm, and about 7 times weaker for the standard geotherm (Fig. 6b).

After about 6 Ma, shortening is responsible for lithospheric thickening and brings the Moho to a depth of 46 km (Figs. 5 and 6a), for both hot and standard geotherms. At this time, an orogenic crustal root develops in the sub-arc/rift domain as the lithology homogeneously thickens and contains a thickened arc/rift geotherm that is about equal to the adjacent continental shoulder geotherm (Figs. 5 and 6). In all cases, the crustal layers of a thickening crustal root remain weaker than the adjacent continental shoulder rocks. The upper crust of the thickening crustal root is slightly stronger than adjacent continental upper crust, but weaker than the adjacent continental lower crust. Similarly, the lower crust of the emerging crustal root is slightly weaker than the shoulder lower crust (Figs. 5 and 6), and is significantly weaker than the upper part of sub-continental mantle.

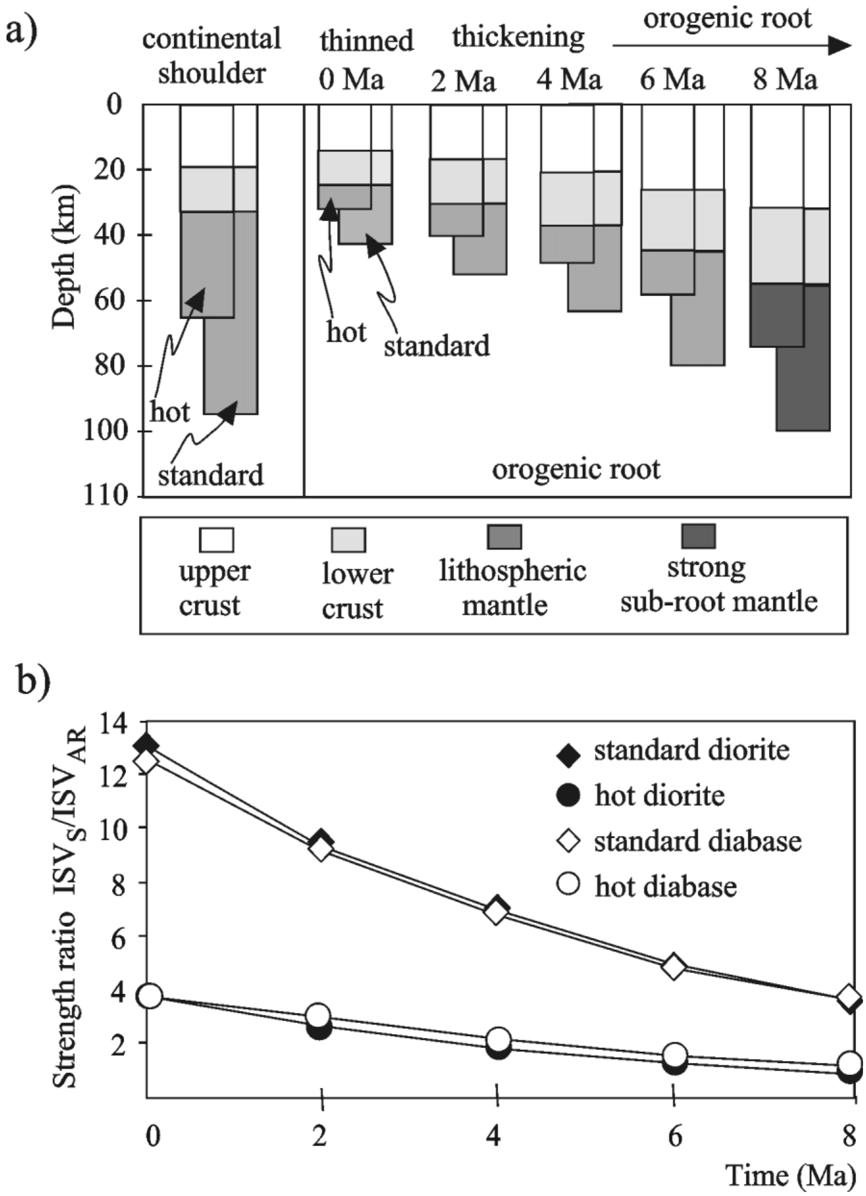


Fig. 6. The evolution of (a) crustal thickness (depth to Moho), and (b) the ratio of $ISV_S$ (shoulder) /$ISV_{AR}$ (arc/rift root), is shown for a history of root thickening during convergence following extensional thinning of an arc (or rift) for unperturbed (S = shoulder) and thinned (AR = arc/rift) continental lithosphere. The cases of felsic = diorite, mafic = diabase lower crustal rheologies (20–35 km depth), for 'hot' and 'standard' geotherms (Table 1), are shown by different symbols, at 2 Ma time intervals (from Fig. 4a and b). The Moho reaches maximum depth (55 km) after about 8 Ma.

At this stage of thickening it is important to note that for the standard geotherm the orogenic crustal root-domain is about 5 times weaker than the adjacent lithosphere, whereas for the hot geotherm the root is about 1.6 times weaker (Fig. 6b). The fact that the layers of the thickened root are either of equal strength or are weaker than adjacent rocks means that the material can still be shortened. This is much more efficient for the standard than for the hot geotherm, because of the much stronger sub-shoulder mantle for the standard geotherm.

In the final stage of the formation of an orogenic root (at about 8 Ma), the Moho reaches a depth of about 55 km (Fig. 6a) and the geotherm of the root domain becomes progressively colder than that of the adjacent continent. Then the sub-root mantle becomes stronger than the lower part of adjacent sub-continental mantle (Fig. 5). In all other parts of the column, the continental shoulder lithosphere is stronger than the crustal root. Thus, even when the thickened root geotherm is colder than that of the adjacent continental lithosphere, the root is still weaker than the adjacent continent.

For the hot geotherm, the strength ratio between both lithospheric domains is small (1.1) suggesting that the crustal root and the adjacent continental lithosphere are equally strong. In contrast, for the standard geotherm the lithospheric strength ratio is still high (3.7), and the sub-root mantle is 10 times stronger than the adjacent sub-continental mantle (Fig. 5).

The fact that the crustal root mantle has become stronger than adjacent continental lithospheric mantle is probably critical for the further mechanical development of the crustal root. This development can be characterised by a depressed geotherm, and an almost equal integrated strength (for a hot geotherm). Alternatively, it is characterised by a weaker root than adjacent continental lithosphere (for standard geotherm), and also by a stronger mantle flooring the thickening crustal root. This emerging root is probably in dynamic equilibrium with the adjacent continental lithosphere (hot geotherm), and is mechanically constrained at the bottom by a stronger mantle layer. Importantly for the standard geotherm, crustal root rocks remain significantly weaker than the continental lithosphere.

### *7.2. Different crustal roots from different initial geotherms*

Two distinct types of behaviour can now be simulated for different crustal roots. For the hot geotherm the root cannot be depressed farther because it has a similar strength to that of the adjacent lithosphere and a stronger floored mantle beneath. For weak remote forces the crustal root is an undeformable lithological heterogeneity. Alternatively, if the remote forces are stronger, the deformation can now propagate into the adjacent continental lithosphere. Because the lithospheric strength is low ($3.7 \times 10^{12}$ and $4.16 \times 10^{12}$ N m$^{-1}$ for the hot geotherm and dioritic and mafic lower crust, respectively), the latter behaviour is likely. The thickened hot geotherm is close (slightly colder) to the stable geotherm of the adjacent lithosphere. Thermal relaxation can be responsible for the further slight weakening of the crustal root. In this case the sub-root mantle reaches equal strength with respect to adjacent sub-continental mantle, whereas the crustal rocks of the continental root become weaker than the adjacent sub-continental mantle and the continental lower crust. These conditions may be favourable for further extrusion of the crustal root.

For the thickened standard geotherm, the crustal root is characterised by a strong sub-root mantle and weak crustal root rocks. This case is not in dynamic equilibrium and converging continental shoulders can further shorten horizontally the crustal root rocks. The whole process of thickening is rapid and a maximum Moho depth of 55 km is reached during 8 Ma. The burial rate is so high that the temperature does not equilibrate during the thickening process, and the isotherms are transported downwards with the rocks. Consequently, the temperature in the sub-root Moho is the same as beneath the arc/rift Moho.

The thickness of the sub-root rigid mantle layer is controlled by the initial pre-extensional and pre-thickening geotherm. After thickening from a hot geotherm, the maximum thickness of a rigid mantle layer flooring the crustal root is only 20 km within the depth range from 56 to 80 km. This means that for a crustal root 56 km thick the underlying and supporting strong mantle layer is quite thin for thickening from a hot geotherm. For a standard geotherm, the thickness of sub-root mantle reaches 90 km which means that the root of 55 km thickness is supported by a mechanically very strong sub-root mantle (Fig. 6a).

## 8. Relative importance of rate of thickening and of thermal relaxation — the time scaling

The thermomechanical evolution during thickening of a previously extended domain is strongly dependent on the cooling history of the lithosphere after

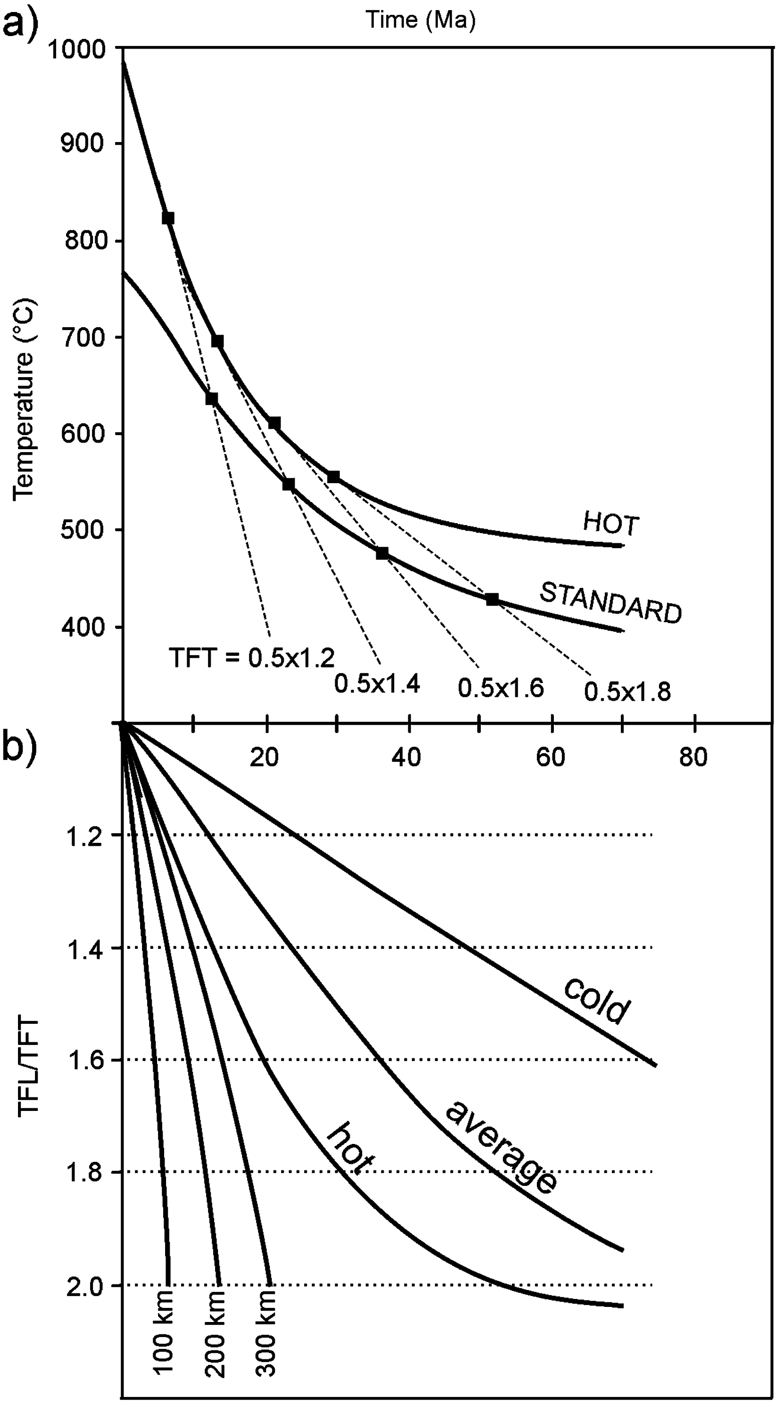


Fig. 7. Cooling and burial histories of root thickening during convergence of continental lithosphere previously thinned by extension in a continental arc or rift. (a) A temperature–time (Ma diagram for the thermal histories of samples at the Moho buried from extension depths of 25 km during relaxation of perturbed standard and hot geotherm. (b) Shows the relative importance of relaxation of hot, standard and cold perturbed geotherms compared to thickening rates of domains 100, 200 and 300 km wide expressed by factors TFT/TFL (initial values TFT = TFL = 0.5 are multiplied stepwise by 1.2).

extension. At the end of tectonic and magmatic activity the cooling lithosphere finally reaches an equilibrium state (Morgan and Ramberg, 1987). The time necessary for conductive cooling is related to the depth of the thermal perturbation and is given by a characteristic thermal response time equal to $l^2/4\kappa$, where $l$ is the depth of perturbation and $\kappa$ is the mean thermal diffusivity (Lachenbruch and Sass, 1978).

In our model we examined hot, standard and cold geotherms with equilibrium lithosphere thicknesses of 66, 90 and 136 km, respectively. Thus, the depth of the thermal perturbation defined by TFT = 0.5, is half of these depths. The numerical solution to the heat conduction equation for relaxation of perturbed geotherms is shown in Fig 7a for samples located at 25 km (thinned Moho). The initial perturbed geotherms were defined by TFT = 0.5, and we show the increase of TFT corresponding to the relaxation. The relaxation of the hot geotherm is faster than of the standard geotherm. So, for example, the multiplication factor 1.4 corresponds to about 15 Ma of cooling for the hot geotherm and about 25 Ma for the standard geotherm.

Likewise, the time scaling of the thickening process (burial) for homogeneous pure shear deformation is obtained from the strain rate. This is controlled by the ratio of the velocity of convergence and the width of the deformed zone (see Appendix A). Extended domains of widths 100 km (narrow zone), 200 and 300 km (wide zones) are homogeneously shortened by orthogonal convergence at an initial velocity of 1 cm/year. The wider the weak region, the slower the rate of thickening and the smaller the increments of vertical motion. These relations have a great effect on the rate of thermal equilibration related to thickening of a former extended domain, especially with a continuous thermal anomaly. Shortening of 100, 200 and 300 km wide extended domains by 1 cm/year, produces double thickness of the rift lithosphere at vertical strain rates of $\dot{\epsilon} = 0.1$, 0.05 and 0.033 $\mathrm{Ma}^{-1}$, after 7, 14 and 21 Ma, respectively.

The scaling of thermal relaxation using TFT and scaling of thickening using TFL, allows us to compare the relative efficiencies of both thermal relaxation and thickening processes with time. Fig. 7b shows the importance of relaxation of three perturbed geotherms compared to thickening of domains 100, 200 and 300 km wide using the factors TFT and TFL. Fig. 7 shows that the cooling is as efficient as thickening for wide extended domains with a perturbed hot geotherm. On the other hand, cooling of perturbed standard and cold geotherms is much slower compared to thickening for any width of deformed rifts. These calculations place upper bounds on thermal relaxation and thickening rate processes.

## 9. Effect of rates of geotherm relaxation and of thickening on strength and depth of orogenic roots

We modelled the thickening during convergence of extended domains of different width (narrow = 100 km, wide = 300 km) as a function of the relaxation of hot and standard perturbed geotherms. In this model, we assume that the boundary representing the depth to which the geotherm will relax moves passively downwards. This is valid only if a heat supply deep in the column has little effect on the thermo-rheological evolution above it.

For constant strain-rate (plate velocity decreases linearly with the width of the deformed zone), the downward motion (burial) is much faster than the thermal relaxation for the standard geotherm and also faster but less fast for the hot geotherm (Fig. 6b). The constant strain rate calculation does not account for any changes in relative strength of shoulders or of the deformed arc/rift zone associated with the thickening process. Thermal hardening is observed to occur as the stronger layers are depressed, thickened, and cooled. This decreases the strain-rate (burial rate) and consequently decreases the velocity of the moving plate. This also inhibits thickening, blocks the system and prevents the formation of any crustal root. Therefore, we also modelled convergence with decreasing strain-rate and hardening. As a limiting case, we assumed that the strain rate drops to zero when the integrated strengths of the shoulder and arc/rift (future root) domains are equal.

The results of calculations for both constant strain rate and thermal hardening are presented in Fig. 8 for narrow zones (100 km) and Fig. 9 for wide zones (300 km). We use depth–temperature diagrams (Figs. 8a and 9a) to show the evolution of a sample initially located (after thinning from 35 km) at the Moho at 25 km; ISV ratio versus time diagrams

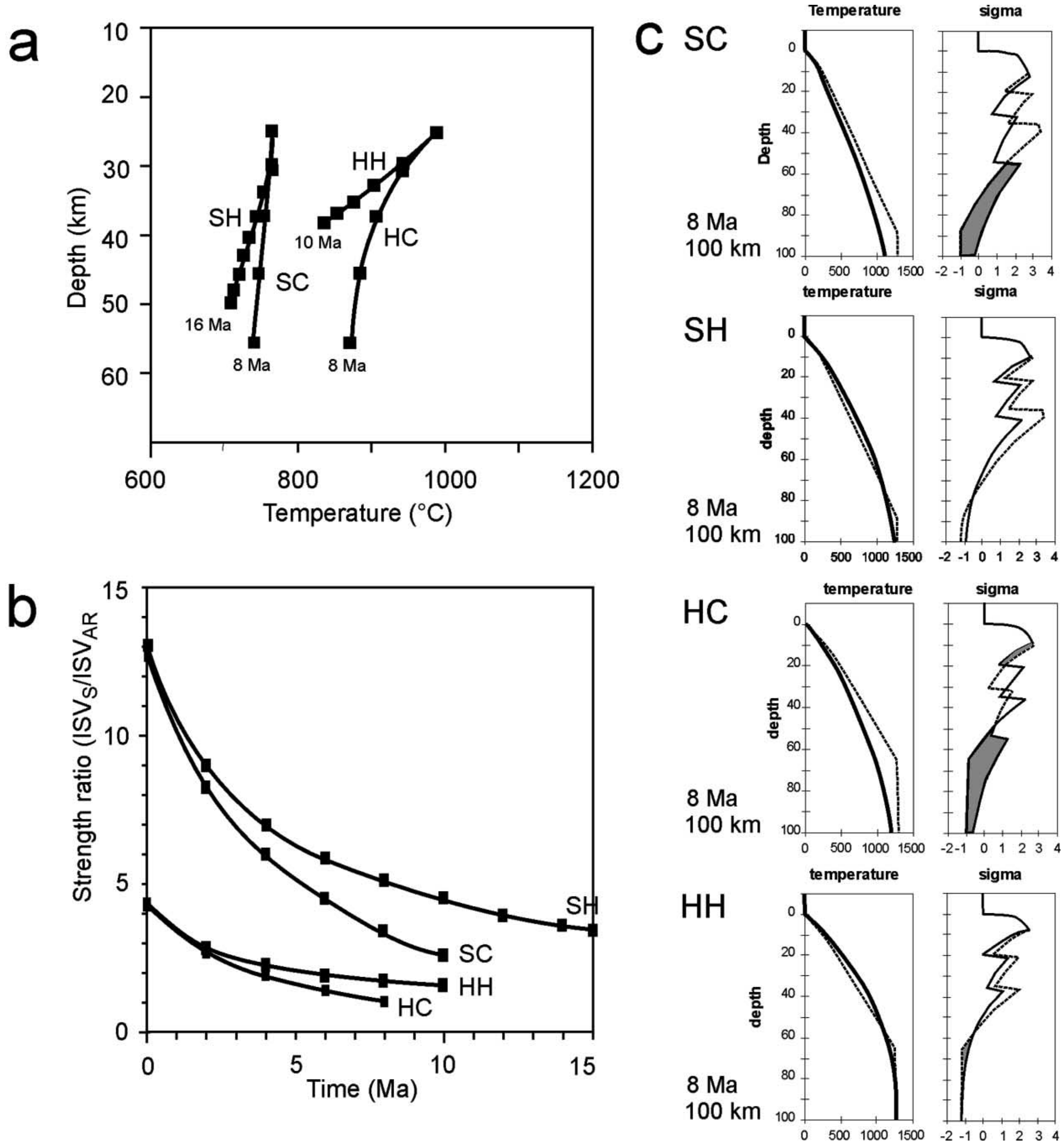


Fig. 8. Burial behaviour during root thickening of continental lithosphere previously thinned by extension in a narrow (100 km) continental arc or rift, as represented by sample initially located (after thinning) at Moho (25 km, $\beta = 1.7$) for two geotherms. The results are presented as (a) depth–temperature diagrams showing also increase of depth to Moho with time, (b) ISV, ratio decrease with time, and (c) geotherms and YSE diagrams calculated after 8 Ma. Curve HH, hot geotherm with thermal hardening, HC, hot geotherm with constant strain rate thickening, SH, standard geotherm with thermal hardening, SC, standard geotherm with constant strain rate thickening.

(Figs. 8b and 9b); and YSE diagrams for 8 and 16 Ma (Figs. 8c and 9c).

Narrow zones (100 km) deforming at constant strain-rate, for both perturbed (hot and standard) geotherms, result in Moho samples at 25 km to be buried to 55 km (Fig. 8a, curves HC and SC). Fig. 8c indicates that the downward movements should stop after 8 Ma due to the development of a stronger mantle layer below the deepening root. This root becomes stronger than the adjacent continental mantle. At this time, the integrated strength of the root has increased to the point where for the hot geotherm the ratio $ISV_S/ISV_{AR} = 1.2$, and for the standard geotherm, $ISV_S/ISV_{AR} = 3.6$. In the case of thermal hardening, the burial rate of a narrow zone slows and the final depth of the root for the standard geotherm can be expected to be 52 km after 16 Ma (curve SH in Fig. 8a) and 37 km after 10 Ma for the hot geotherm (curve HH in Fig. 8a). A surprisingly shallow depth of the thickened domain results for the hot geotherm because of very efficient thermal hardening associated with cooling (from 1000°C at 25 km to 820°C at 37 km).

Wide zones (300 km) deforming at constant strain rate by thickening from both perturbed hot and standard geotherms, result in Moho samples at 25 km to be buried to nearly 45 km because of the development of a hard sub-root mantle layer and a significant increase in sub-root lithospheric strength. This occurs after 16 Ma of burial for both standard and hot geotherms ($ISV_S/ISV_{AR} = 3.6$, $ISV_S/ISV_{AR} = 1.5$, respectively). Thickening associated with thermal hardening of wide zones for hot and standard geotherms finishes at shallow burial levels (30, 35 km, respectively) and therefore cannot produce any crustal root. This happens at different times for standard and hot geotherms which become hard at 35 km after 20 Ma (SH), at 30 km after 16 Ma (HH); with ($ISV_S/ISV_{AR} = 3.6$) and ($ISV_S/ISV_{AR} = 1.8$), respectively (Fig. 9a and b).

Thus, 100 km wide zones are buried deeper and quicker than 300 km-wide zones for both constant strain rate and thermal hardening cases. Because the hot geotherm relaxes faster than the standard geotherm, hardening occurs at shallower levels. For zones of any width, the depressed and relaxed root and shoulder geotherms are almost the same in the upper 50 km. In the final stage of thickening, the sub-root mantle is several times stronger than the sub-shoulder mantle, but the root lower and upper crust are weaker than the adjacent shoulder mantle and lower crust. The downward blocking of the root at different depths in the various models potentially leads to decoupling above the Moho and hence to horizontal shortening of the crustal root by the stronger converging shoulder.

### *9.1. Effect of heat addition during thickening on the formation of an orogenic root*

The previous cases of constant strain rate and thermal hardening represent two probable limiting cases. The former case represents a thickening process in which rheological changes are fully neglected, and the latter case shows the maximum influence of cooling on rheology but does not include the effects of advected heat from the mantle. However, we can assume that the thermal anomaly corresponding to the initially uncoupled thinning (of thermal and lithological structure) does not cease but continues to be active during thickening. In our models, this additional heat flows in the opposite direction (upwards) to the growth of the root (downwards).

We have attempted to simulate the thickening of extended domains with perturbed geotherms in which cooling is retarded because of an added heat supply. This can be achieved mathematically by placing the lithosphere–asthenosphere thermal boundary layer close to the initial Moho depth and keeping it there throughout the convergence and thickening (see Fig. 9a–c). This effect would be maximised for the case of a hot mantle magma penetrating upwards through thickening crust descending in a compressive regime. This results in a greater vertical length of weak zones and permits increased amounts of deepening of the Moho for any thickening rate. Furthermore, the intensity of thermal hardening may be considered to occur between previous constant strain-rate and thermal hardening cases. The results of these calculations are shown in Fig. 10. Even though we find it difficult to visualise the mechanics of such a process of intrusion during thickening on the 100 km length scales considered here, a natural examples on smaller scale include parts of the Appalachians (Brown and Solar, 1998).

For narrow zones (100 km), with both perturbed geotherms (hot and standard), the burial proceeds to

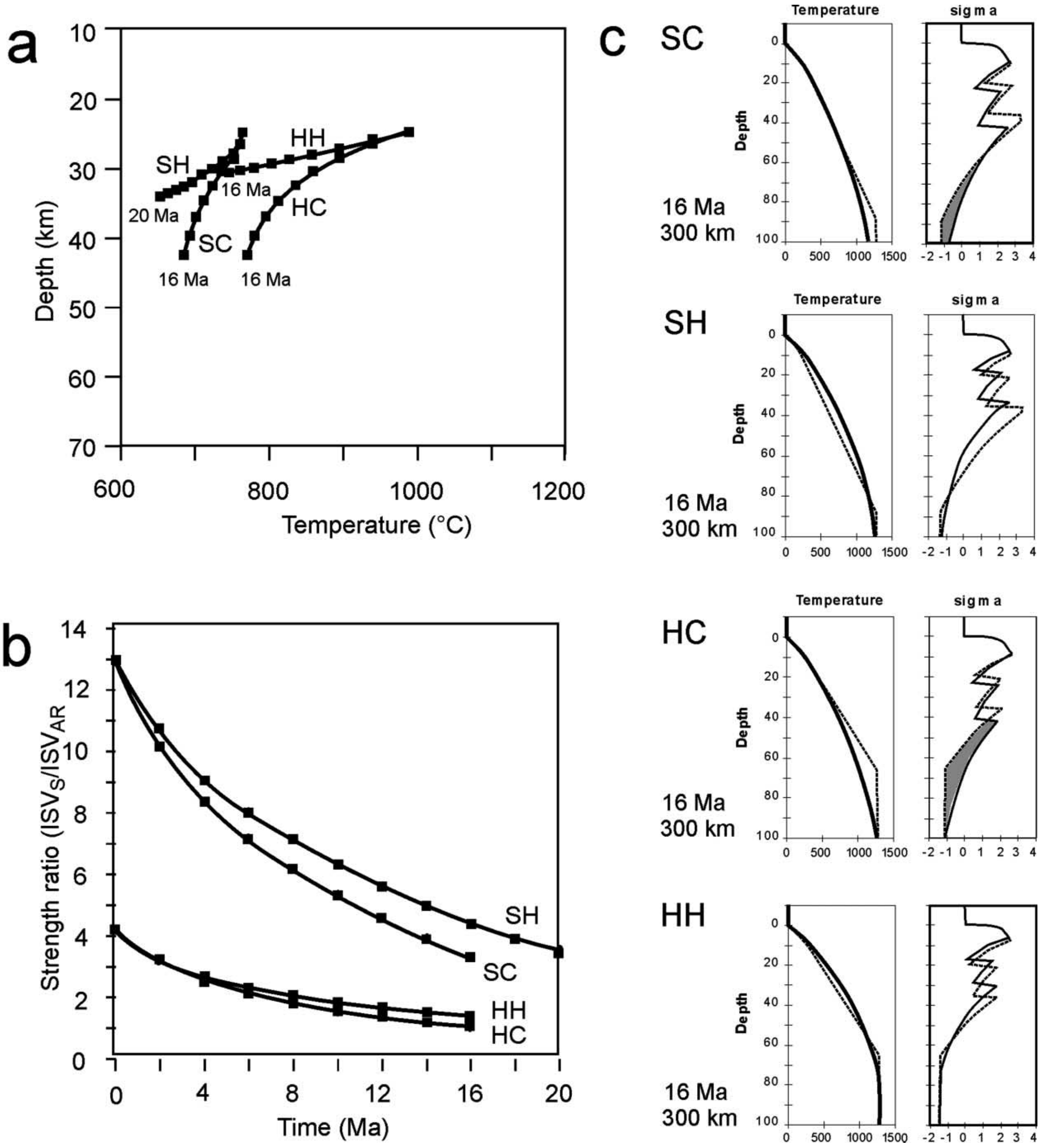


Fig. 9. Burial behaviour during root thickening of continental lithosphere previously thinned by extension in a wide (300 km) continental arc, or rift, as represented by sample initially located (after thinning, $\beta = 1.7$) at Moho at 25 km. The results are presented as (a) depth–temperature (b) ISV, ratio decrease with time, and (c) geotherms and YSE diagrams calculated for the maximum depth of the Moho after 16 Ma. Gradual hardening throughout the column decreases plate velocity to zero. Curve labelling as in Fig. 8.

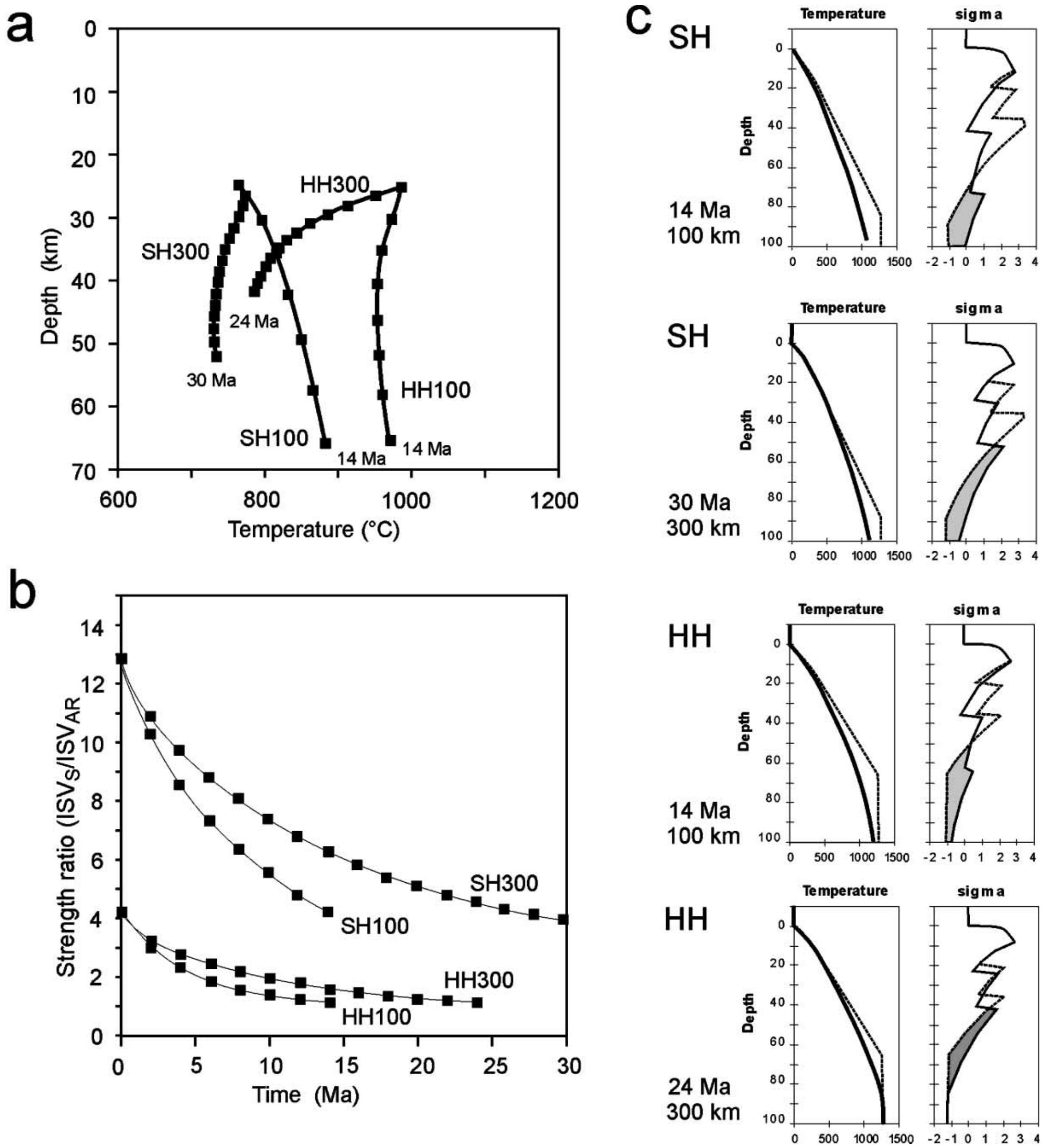


Fig. 10. Effect of heat addition during thickening of continental lithosphere previously thinned by extension in a narrow (100 km) and wide (300 km) continental arc, or rift for both standard and hot geotherms. The results are presented as (a) depth–temperature diagram (b) ISV, ratio decrease with time diagram, and (c) geotherms and YSE diagrams calculated for the maximum depth of the Moho after 14 Ma for narrow zone and 24, 30 Ma for wide zone. Curve labeling as in Figs. 8 and 9.

depths close to 60–70 km (Fig. 10a, curves HH100 and SH100). There a hard layer of sub-root mantle develops after about 14 Ma. Thermal hardening occurs, so that at the end of burial the strength ratio $ISV_S/ISV_{AR} = 4$ and $ISV_S/ISV_{AR} = 1.5$ for standard and hot geotherms, respectively. For wide zones (300 km), the crust attains a thickness of 40 km for the hot geotherm and 52 km for the standard geotherm, respectively. The downward movements are much slower (>30 Ma) due to a progressive decrease of strength ratio between the root and shoulder (Fig. 10b).

## 10. PT evolutions during burial in deepening orogenic roots

The thermal histories here strongly reflect an extensional phase that includes heating prior to convergent thickening. In contrast, burial (thickening) of terrains with normal (non-extended) crustal thickness and cold to average thermal structure (such as subduction zones and zones of underthrusted continental plates), will result in increase of the depressed geotherm due to heating by the adjacent mantle, sometimes supplemented by radioactive heat production in the crust.

Several types of burial PT paths were produced in this study. In Figs. 8a, 9a and 10a we tracked the burial histories of samples located at the Moho from an initial depth after thinning of 25 km. First, at constant strain-rate without thermal relaxation, almost isothermal burial paths were obtained, with very high burial rates (8 Ma) to a maximum burial depth of 60 km. Second, at constant strain-rate but with decreasing plate convergence velocity, and with associated thermal relaxation, the depth and rate of burial strongly depends on the width of the orogenic zone (100 km width, 8 Ma from 25 to 55 km; 300 km width, 16 Ma from 25 to 45 km). Because of some thermal relaxation, these samples show about 100°C of cooling during this burial history for the standard geotherm and 200°C for the hot geotherm (Figs. 8a and 9a). Third, the histories with decreasing strain-rate and decreasing plate velocities show slow burial rate and shallow depth of burial due to thermal hardening especially for wide orogenic zones. For 300 km-wide zones, models with both geotherms show limited deepening of the Moho to 35 and 30 km (by 10 km for the standard geotherm and 5 km for the hot geotherm). This is accompanied by a decrease in temperature of 340°C (after 16 Ma) for the hot geotherm, and 170°C (after 20 Ma) for the standard geotherm. The PTt diagram in Fig. 9 shows cooling during burial and indicates possible burial paths from the high-temperature/low-pressure (HT/LP) type of metamorphism to low-temperature/medium-pressure (MT/LP–MP) conditions.

For 100 km-wide zones with a standard geotherm, the Moho sample is buried from 25 km down to 52 km while undergoing 60°C of cooling over 16 Ma (Fig. 8). In contrast, the hot geotherm Moho sample is buried from 25 to 38 km over 10 Ma and undergoes cooling of 200°C. For an initially hot geotherm, the temperature at the Moho after thickening reaches a maximum of 800°C. This, in turn, indicates that only a narrow layer of medium-pressure–temperature (MP/MT) eclogites could originate during the thickening phase. Thermal equilibration may produce granulitization of such eclogites at MP conditions.

Fourth, additionally supplied heat will heat the adjacent rocks by contact metamorphism faster than the whole column cools by regional, downward advective cooling (Fig. 10). Characteristic features for narrow zones are PTt paths that show heating with burial for a standard geotherm and an almost isothermal evolution for a hot initial geotherm. In such a case, HT/HP metamorphism can develop hot-eclogites (from the standard geotherm) and HP-granulites (for the hot geotherm) because the maximum depth of thickening is 60 to 70 km. This evolution is due to the competition between efficient cooling during burial of a perturbed hot initial geotherm and the additional heating from below. For wide zones, very limited cooling and burial down to 53 km is observed from a standard initial geotherm and cooling of about 220°C is associated with burial to 43 km for a hot initial geotherm (Fig. 10). This induces a MP/MT metamorphism. PTt paths for both cases are counterclockwise and involve significant amounts of cooling. An MP/MT metamorphic gradient is expected for these evolutions.

## 11. Multistage and successive events in orogenic development

We have shown that the development of progressive tectonic domains strongly depends on the uplift of the thermal regime during thinning of lithological layering preceding the convergent thickening of crustal weak zones. When thermal and lithological structures are coupled during thinning immediately prior to thickening, convergence closely following this extension and thinning cannot easily depress the Moho, and no orogenic root forms. Uncoupled thermal and lithological thinning during this earlier extensional phase, with additional heat input, is needed to soften this sub-arc/rift mantle such that in later convergence the paleo-arc/rift domain can thicken to form an orogenic root.

To produce a deep orogenic root in non-softened continental crust is difficult. In order to produce an orogenic root in previously softened continental crust thinned by extension, the thermal structure and lithospheric thinning need to be decoupled, i.e. convergence must be fast. The depth of the transposed Moho depends on the thermal evolution during thickening and can be located at depths of 60 km, irrespective of the type of initial geotherm. This is the typically reported depth to Moho beneath orogenic roots (Jarchow and Thompson, 1989; LePichon et al., 1997). Our important result is that primarily the rheological hardening of both the crustal root and underlying mantle controls the actual depth of blocking of a deepening orogenic root in the mantle during multistage and successive orogenic events. If continental convergence starts soon after the thinning event has ceased, or if the arc/rift is continuously heated by long lived or continued magmatic events, then the continental convergence results in production of an orogenic root by homogeneous thickening (with the present simplified rheological model in the sense of LePichon et al., 1997, Fig. 3; or Ziegler et al., 1998, Fig. 1).

Thompson (1989a,b) concluded that the wide orogenic zones of the Canadian Slave Province exhibit only moderate thickening of previously heated and extended lithosphere (as also suggested for the Acadian Appalachian orogeny, e.g. Brown and Solar, 1998). Our models provide time constraints and rheological explanations for these important orogenic events. In contrast to proposed thermal histories for continental collision zones considered to date, the rocks in our multistage metamorphic evolution cool down during burial because they retain a thermal memory of their extension. The thermal considerations here of the period following blocking of root formation by the hardening of the mantle, and hence the end of thickening, show that this lasts for about 10 Ma when thermal hardening is not taken into account, and between 20 and 30 Ma when rocks harden during burial. This time-lag is therefore important in order to permit the cooled buried rocks to heat and soften again, so that they are exhumed by vertical extrusion during lateral compression. This study also shows that thickening is only possible when the sub-arc/rift rocks are weaker than the adjacent continent in the whole vertical column. Furthermore, the maximum depth of the orogenic root is attained when the sub-root mantle becomes stronger than sub-continental mantle adjacent to the weak zone, and when the integrated strengths of both domains become similar.

## 12. Conclusions

Our study has shown that thinned crustal zones are potentially suitable domains for development of future crustal orogenic roots. For an orogenic root to be produced by thickening of previously softened continental crust thinned by extension, the thinning of isotherms must have been greater than thinning of the lithologies. This necessitates an external heat input additional to simple thinning of isotherms following extension. We suppose that this supplementary heat source is represented by upwelling of the asthenospheric mantle, which may further undergo decompressional melting, and may result in massive injection of mafic magmas into the lower crust. Another possibility is a long-lived heat source below an arc or rifted domain represented by a stable plume of mantle material.

Our conclusions may be summarised for arc/rift zones where lithological and thermal structures remain ‘coupled’:

(1) The sub-arc/rift mantle may become so strong that it cannot be deformed by subsequent convergence of the approaching continent, which is weaker.

(2) The sub-arc/rift mantle is stronger than, and can indent the lower crust of, an adjacent converging continental shoulder.

(3) No root can be produced in such a sub-arc/rift mantle by later convergence towards the extended domains. If anything, the thinned arc/rift will be isolated by the collision of converging continental shoulders.

Thus a 'failed' rift or arc will be shut-off by later impingement of continental shoulders. During this phase metamorphic core complexes can be formed and/or excavated.

For extended zones where lithological and thermal structures are 'un-coupled'.

(4) A mechanism is provided in 'failed' rifts or arcs to enable 'orogenic roots' to form in soft zones that can become thickened during subsequent continental convergence.

(5) Decoupled lithological and thermal thinning produce a shallow root with a maximum depth of 60 km. No ultrahigh pressure (UHP) rocks are generated or exhumed here.

(6) Granulites and metamorphic assemblages typical of HT/LP terrains are formed during lithospheric thinning. Subsequent thickening during convergence leads to medium-temperature MT-eclogites for the thickened geotherms of narrow zones and high-temperature (HT or 'hot') eclogites when the previous narrow arcs or rifts become heated during thickening. An important feature is that limited thickening and strong cooling of wide arc/rift zones leads to LP/LT metamorphism. These $P$–$T$ paths are counter-clockwise.

(7) When thick lithosphere (with a cold initial geotherm) is thinned and then thickened it can reach a thickness of 55 km. When thin lithosphere (with a hot initial geotherm) is thinned and then thickened it cools very rapidly and hardens exceptionally quickly (<10 Ma).

(8) If additional heat enters during thickening (continuous magmatism), then root thickening of up to 60–70 km can occur and can lead to the formation of hot eclogites.

(9) The examples discussed here are for two-sided (but not necessarily symmetrical) thinning/thickening of soft intra-continental zones, or back-arc basins. They are not specifically applicable to one-sided subduction against continental macro plates (LePichon et al., 1997).

## Acknowledgements

The Czech National Foundation grant No. 205/98/K004, the Grant Agency of Charles University grant No. 296/1997/B GEO, the Schweizerische National Fonds and ETH Research credits, are gratefully acknowledged for financial support. We are especially grateful to Mark Handy and an anonymous reviewer for very constructive reviews, and to Wolfgang Franke for acting as editor.

## Appendix A

A simple 1D model to investigate thermomechanical properties of the lithosphere

In many recent studies, the properties of the lithosphere, especially with respect to response to lateral forces, have been described in terms of yield strength envelopes (YSE) that enable a comparison of relative resistance to deformation of lithospheric layers. The whole lithosphere strength is then characterised by the integrated strength value (ISV). The YSE are typically computed as a strength needed for a permanent deformation. For a brittle deformation, a Navier–Coulomb Law with Byerlee's constants (Byerlee, 1978) is used:

$$\sigma = \beta \rho g z (1 - \lambda) \tag{A1}$$

where $\sigma$ is differential stress, $\beta$ the parameter for type of faulting, $\rho$ the density, $g$ the gravity acceleration, $\lambda$ the pore fluid factor, and $z$ the depth.

For ductile deformation we consider creep strength:

$$\sigma = (\dot{\epsilon}/A)^{1/n} \exp\left(\frac{Q}{n\mathrm{R}T}\right) \tag{A2}$$

where $\sigma$ is the differential stress, $\dot{\epsilon}$ the strain rate, $A$ the Dorn parameter, $n$ the stress exponent, $Q$ the creep activation energy, R the gas constant, and $T$ the temperature. The YSE value at any given depth is the lesser of the brittle and ductile differential stresses.

Our basic evaluation of a potential evolution of a selected domain consists of a comparison of YSE and ISV of neighbouring units (e.g. arc, rift or orogenic root versus continental shoulder) that is controlled by rheological parameters and temperature profiles in Eqs. (A1) and (A2). Possible lithospheric layering and temperature profiles supply an infinite variety of combinations that, nevertheless, can be categorised by a low number of typical situations. In order to simplify this categorization we choose only one reference lithological profile (e.g. the first 20 km of quartz, then 15 km of diorite or diabase, and olivine below) and one reference vertical temperature profile (e.g. a

Table A1
Time correspondence of the TFL (thickening/thinning factor of lithology) for $\dot{\epsilon} = 0.1\ \mathrm{My}^{-1}$

| TFL | 1.0 | 1.1 | 1.2 | 1.3 | 1.4 | 1.5 | 1.6 | 1.7 | 1.8 | 1.9 | 2.0 |
|---|---|---|---|---|---|---|---|---|---|---|---|
| Time (Ma) | 0.0 | 0.95 | 1.82 | 2.62 | 3.36 | 4.05 | 4.70 | 5.31 | 5.88 | 6.42 | 6.93 |

typical cold, mean = standard, or hot geotherm, Table 1). All the other lithologies/temperature profiles we derive from the reference profiles by means of two factors that we call the thickening/thinning factor of lithology (TFL) and thickening/thinning factor of temperature (TFT). These factors control the rescaling of the vertical depth axis, so that the values TFL, TFT > 1 correspond to thickening and TFL, TFT < 1 to thinning. This rescaling of the depth axis can also be complemented by a shift corresponding to isostatic compensation.

The parametrization of the lithology and temperature profiles by the factors TFL, TFT can approximate typical orogenic events. For example, the case TFL = TFT = 2 would correspond to an instantaneous double homogeneous thickening of the lithosphere without any heat exchange (e.g. an orogenic root), while the case TFL = 0.7 and TFT = 0.5 indicate thinned lithology (e.g. a rift) with anomalous heat flow. In both cases we can compute YSE and ISV and compare them to YSE and ISV of the reference lithology/temperature profiles of shoulders adjacent to the thickened/thinned domain (which formally correspond to TFL = TFT = 1), and then we can examine orogenic consequences.

By changing values of the factors TFL, TFT stepwise we can simulate a time evolution of a domain under consideration. For example, a stepwise multiplication of values of TFL and TFT by a factor 1.1 would correspond to gradual thickening of the lithosphere together without thermal relaxation. An approximate relation of TFL to geologic time is given by the strain rate of the geological processes. If we consider a homogeneous deformation of a zone of initial width $d$ by plates approaching with an initial velocity $v$, then the strain rate $\dot{\epsilon} = v/d$. Provided that the strain rate is constant during deformation, the corresponding time is:

$$t = \frac{\log(\mathrm{TFL})}{\dot{\epsilon}} = \log(\mathrm{TFL})d/v \tag{A3}$$

From Table A1, which is computed for the case of homogeneous deformation of a 100 km wide zone by a velocity of 1 cm/year, i.e. the strain rate $\dot{\epsilon} = 0.1\ \mathrm{My}^{-1}$, we find that about 7 My corresponds to TFL = 2.

The time correspondence of TFT can be established by numerical modelling of thermal relaxation and it is basically given by conductive thermal response time of the upper parts of lithosphere, that is by the thermal diffusivity. As an example, in Table A2 we bring values of TFT corresponding approximately to the thermal relaxation of a rift (we computed them as slopes of the nearly linear parts of relaxing geotherms in the 1D model in Fig. 1. of Morgan and Ramberg, 1987). As discussed, the thermal conductive relaxation is much slower and therefore the times corresponding to TFT are longer, e.g. for TFT = 2 the time is about 35 My.

Our first investigations were based on examination of a large number of combinations of the factors TFL and TFT justified by the fact that particular combinations of lithology and temperature must occur during orogenic processes (as transitory phases) and we do not need to use a complex modelling to examine them. In a second step, we improved our estimations by considering conductive relaxation of geotherms sometimes with additional heat supply from the mantle.

Table A2
Time correspondence of the TFT (thickening/thinning factor of temperature) for a hot geotherm

| TFT | 1.0 | 1.1 | 1.2 | 1.3 | 1.4 | 1.5 | 1.6 | 1.7 | 1.8 | 1.9 | 2.0 |
|---|---|---|---|---|---|---|---|---|---|---|---|
| Time (Ma) | 0.0 | 2.68 | 5.50 | 8.47 | 11.62 | 14.94 | 18.44 | 22.14 | 26.05 | 30.17 | 34.52 |

## References


Allemand, P., Brun, J-P., 1991. Width of continental rifts and rheological layering of the lithosphere. Tectonophysics 188, 63–69.

Bassi, G., Keen, C.E., Potter, P., 1993. Contrasting style of rifting: models and examples from the western Canadian margin. Tectonics 12, 639–655.

Bertotti, G., ter Voorde, M., Cloethingh, S., Picotti, V., 1997. Thermo-mechanical evolution of the South-alpine rifted margin (N-Italy): Constraints on the strength of passive continental margin. Earth Planet. Sci. Lett. 146, 181–193.

Brown, M., Solar, G., 1998. Granite ascent and emplacement during contractional deformation in convergent orogens. J. Struct. Geol. 20, 1365–1393.

Buck, W.R., Toksoez, M.N., 1983. Thermal effects of continental collisions: thickening a variable viscosity lithosphere. Tectonophysics 100, 53–69.

Cermák, V., Bodri, L., Schulz, R., Tanner, B., 1993. Crustal temperatures along central segment of the European lithosphere. Tectonophysics 195, 241–251.

Chery, J., Vilotte, J.P., Daigniers, M., 1991. Thermomechanical evolution of a thinned continental lithosphere under compression: Implications for the Pyrenees. J. Geophys. Res. 96, 4385–4412.

Cloethingh, S., van Wees, J.D., van der Beek, P.A., Spadini, G., 1995. Role of pre-rift rheology in kinematics of extensional basin formation: constraints from thermomechanical models of Mediterranean and intracratonic basins. Mar. Pet. Geol. 12, 793–807.

Cloetingh, S., Burov, E.B., 1996. Thermomechanical structure of European continental lithosphere: contraints from rheological profiles and EET estimates. Geophys. J. Int. 124, 695–723.

Cosgrove, J., 1997. The influence of mechanical anisotropy on the behaviour of the lower crust. Tectonophysics 280, 1–14.

Dewey, J.F., Burke, K.C.A., 1973. Tibetan, Variscan, and Precambrian basement reactivation: Products of continental collision. J. Geol. 81, 683–692.

Ellis, M., 1988. Lithospheric strength in compression: initiation of subduction, flake tectonics, foreland migration of thrusting, and an origin of displaced terranes. J. Geol. 96, 91–100.

England, P.C., 1987. Diffuse continental deformation: length scales, rates and metamorphic evolution. Tectonic setting of regional metamorphism, Oxburgh, E.R., Yardley, B.W.D., England, P.C. (Eds.), Philos. Trans. R. Soc. London A 321, 3–22.

England, P.C., Houseman, G., 1985. Role of lithospheric strength heterogeneities in the tectonics of Tibet and neighbouring regions. Nature 315, 297–301.

England, P.C., Thompson, A.B., 1984. Pressure–temperature–time paths of regional metamorphism. Part I: heat-transfer during the evolution of regions of thickened continental crust. J. Petrol. 25, 894–928.

Glahn, A., Granet, M., et le groupe téléseismique du Graben du Rhin, 1993. Southern Rhine graben: small-wavelength tomographic study and implications for the dynamic evolution of graben. Geophys. J. Int. 113, 399–413.

Goetze, C., Evans, B., 1979. Stress and temperature in the bending lithosphere as constrained by experimental rock mechanics. Geophys. J. R. Astron. Soc. 59, 463–478.

Green, D.H., 1991. The Earth's lithosphere and asthenosphere concepts and constraints derived from petrology and high pressure experiments. In: Drummond, B.J. (Ed.), The Australian Lithosphere. Geological Society of Australia Special Publication, vol. 17, pp. 1–22.

Grocott, J., Brown, M., Dallmeyer, R.D., Taylor, G.K., Treloar, P.J., 1994. Mechanisms of continental growth in extensional arcs: an example from the Andean plate-boundary zone. Geology 22, 391–394.

Handy, M., 1989. Deformation regimes and the rheological evolution of fault zones in the lithosphere; the effects of pressure, temperature, grain-size and time. Tectonophysics 163, 119–152.

Hopper, J.R., Buck, W.R., 1998. Styles of extensional decoupling. Geology 26, 699–702.

Jarchow, C.M., Thompson, G.A., 1989. The nature of the Mohorovic'ic' discontinuity. Annu. Rev. Earth Planet. Sci. 17, 475–506.

Jamieson, R.A., Beaumont, C., Fullsack, P., Lee., B., 1998. Barrovian regional metamorphism: where's the heat? In: Treloar, P.J., O'Brien, P.J. (Eds.), What Drives Metamorphism and Metamorphic reactions? Geological Society of London, Special Publication, vol. 138, pp. 23–51.

Kirby, S.H., 1983. Rheology of the lithosphere. Rev. Geophys. Space Phys. 21, 1458–1487.

Kooi, H., Cloetingh, S., 1989. Some consequences of compressional tectonics for extensional models of basin subsidence. Geol. Rund. 78, 183–195.

Kusznir, N.J., Park, R.G., 1986. Continental lithosphere strength: the critical role of lower crustal deformation. In: Dawson, J.B., Carswell, D.A., Hall, J., Wedepohl, K.H. (Eds.), The Nature of the Lower Continental crust. Geological Society of London, Special Publication, vol. 24, pp. 79–93.

Lachenbruch, A.H., Sass, J.H., 1978. Models of an extending lithosphere and heat flow in the Basin and Range province. Geol. Soc. Am Mem. 152, 209–250.

Lachenbruch, A.H., Sass, J.H., Galanis, S.P.R., 1985. Heat flow in southern California and the origin of the Salton Trough. J. Geophys. Res. 90, 6709–6736.

Lankreijer, A., Monacu, V., Cloetingh, S., 1997. Lateral variations in lithosphere strength in the Romanian Carpathians: constraints on basin evolution. Tectonophysics 272, 269–290.

LePichon, X., Henry, P., Goffe, B., 1997. Uplift of Tibet: from eclogites to granulites — implications of the Andean plateau and the Variscan belt. Tectonophysics 273, 57–76.

McDowell, S.D., Elders, W.A., 1983. Allogenic layer silicate minerals in borehole Elmore 1, Salton Sea geothermal field, California. Am. Mineral. 68, 1146–1159.

McKenzie, D., 1978. Some remarks on the development of sedimentary basins. Earth Planet. Sci. Lett. 40, 25–32.

Merle, O., Guillier, B., 1989. The building of the Central Swiss Alps: an experimental approach. Tectonophysics 165, 41–56.

Morgan, P., Ramberg, I.B., 1987. Physical changes in the lithosphere associated with thermal relaxation after rifting. Tectonophysics 143, 1–11.

Oxburgh, E.R., 1982. Heterogeneous lithospheric stretching in early history of orogenic belts. In: Hsu, K.J. (Ed.), Mountain Building Processes, 95. Academic Press, London, pp. 85–95.

Parsons, T., Thompson, G.A., Sleep, N.H., 1992. Host rock rheology controls on the emplacement of tabular intrusions: Implications for underplating of extending crust. Tectonics 11, 1348–1356.

Paterson, M.S., Luan, F.C., 1990. Quartzite rheology under geological conditions. In: Knipe, R.J., Rutter, E.H. (Eds.), Deformation Mechanisms, Rheology and Tectonics. Geological Society Special Publication, vol. 54, pp. 299–307.

Quinlan, G., 1988. The thermal signatures of tectonic environments. In: Nisbet, E.G. Fowler, C.M.R. (Eds.), Heat Metamorphism and Tectonics. Mineralogical Association of Canada, vol. 14, pp. 213–257.

Ranalli, G., 1986. Rheology of the Earth. Allen and Unwin, London (366 pp.).

Ranalli, G., Murphy, D.C., 1987. Rheological stratification of the lithosphere. Tectonophysics 132, 281–295.

Royden, L., 1996. Coupling and decoupling of crust and mantle in convergent orogens: Implications for strain partitioning in the crust. J. Geophys. Res. 101, 17,679–17,705.

Schmid, S.M., Handy, M.R., 1991. Towards a genetic classification of fault rocks: geological usage and tectonophysical implications. In: Mueller, D.W., McKenzie, J.A., Weissert, H. (Eds.), Controversies in Modern Geology. Academic Press, London, pp. 95–110.

Sengor, C., Burke, K., 1978. Relative timing of rifting and volcanism on Earth and its tectonic implications. Geophys. Res. Lett. 5, 419–421.

Tatsumi, Y., Kimura, N., 1991. Backarc extension versus continental breakup: petrological aspects for active rifting. Tectonophysics 197, 127–137.

Thompson, P.H., 1989a. Moderate overthickening of thinned sialic crust and the origin of granitic magmatism and regional metamorphism in low-*P*–high-*T* terranes. Geology 17, 520–523.

Thompson, P.H., 1989. An empirical model for metamorphic evolution of the Archaean Slave Province and adjacent Thelon Tectonic Zone, north western Canadian Shield. In: Daly, J.S., Cliff, R.A. and Yardley, B.W.D. (Eds.), Evolution of Metamorphic Belts. Geological Society of London Special Publication, vol. 43, pp. 245–263.

Thompson, R.N., Gibson, S.A., 1994. Magmatic expression of lithospheric thinning across continental rifts. Tectonophysics 233, 41–68.

Tommasi, A., Vauchez, A., 1997. Complex tectono-metamorphic patterns in continental collision zones: the role of intraplate rheological heterogeneities. Tectonophysics 279, 327–350.

Vauchez, A., Tommasi, A., Barruol, G., 1998. Rheological heterogeneity, mechanical anisotropy and deformation of the continental lithosphere. Tectonophysics 296, 61–86.

Ziegler, P.A., Cloetingh, S., van Wees, J.-D., 1995. Dynamics of intra-plate compressional deformation: the Alpine foreland and other examples. Tectonophysics 252, 7–59.

Ziegler, A., van Wees, J.-D., Cloetingh, S., 1998. Mechanical controls on collision-related compressional intraplate deformation. Tectonophysics 300, 103–129.